Global Ecology and Biogeography

A Mac

Spatiotemporal patterns of tree growth as related to carbon isotope fractionation in European forests under changing climate

Journal:	*Global Ecology and Biogeography*
Manuscript ID	GEB-2018-0520.R1
Manuscript Type:	Research Papers
Keywords:	carbon isotopes, climate change, dendroecology, drought stress, European forests, latitudinal gradients, Pinus, Quercus, stomatal control, tree rings

Spatiotemporal patterns of tree growth as related to carbon isotope fractionation in European forests under changing climate

Running head: Ecophysiology of forest growth in Europe

Abstract

Aim

To decipher Europe-wide spatiotemporal patterns of forest growth dynamics and their associations with carbon isotope fractionation processes inferred from tree rings as modulated by climate warming.

Location

Europe and North Africa (30–70°N, 10°W–35°E).

Time period

1901–2003.

Major taxa studied

Temperate and Euro-Siberian trees.

Methods

We characterize changes in the relationship between tree growth and carbon isotope fractionation over the 20th century using a European network consisting of 20 site chronologies. Using indexed tree-ring widths (TRW_i), we assess shifts in the temporal coherence of radial growth across sites (synchrony) for five forest ecosystems (Atlantic, Boreal, cold continental, Mediterranean and temperate). We also examine whether TRW_i shows increased coupling with leaf-level gas exchange, inferred from indexed carbon isotope discrimination of tree-ring cellulose ($\Delta^{13}C_i$).

Results

We find spatial autocorrelation for TRW_i and $\Delta^{13}C_i$ extending over up to 1,000 km among forest stands. However, growth synchrony is not uniform across Europe, but increases along a latitudinal gradient concurrent with decreasing temperature and evapotranspiration. Latitudinal relationships between TRW_i and $\Delta^{13}C_i$ (changing from negative to positive

southwards) point to drought impairing carbon uptake via stomatal regulation for water saving occurring at forests below 60°N in continental Europe. A rise in forest growth synchrony over the 20th century together with increasingly positive relationships between TRW_i and $\Delta^{13}C_i$ indicate intensifying drought impacts on tree performance. These effects are particularly noticeable in drought-prone biomes (Mediterranean, temperate and cold continental).

Main conclusions

At the turn of this century, convergence in growth synchrony across European forest ecosystems is coupled with coordinated warming-induced drought effects on leaf physiology and tree growth spreading northwards. Such a tendency towards exacerbated moisture-sensitive growth and physiology could override positive effects of enhanced leaf intercellular CO_2 concentrations, possibly resulting in Europe-wide declines of forest carbon gain in the coming decades.

Keywords: carbon isotopes, climate change, dendroecology, drought stress, European forests, latitudinal gradients, *Pinus*, *Quercus*, stomatal control, tree rings

Introduction

Understanding the physiological mechanisms underlying variations in forest productivity is a key priority in global change research. Factors such as tree age, forest structure and management, nutrient availability, pollution, etc., influence the carbon budget of forested areas. During the last decades, however, climate change and increased atmospheric CO_2 ($_{atm}CO_2$) have largely altered the productivity of European forests (Nabuurs et al., 2013). To explore these dynamics, research efforts have been usually confined to local ecosystems, with some representative woody species and their interactions examined at small spatial scales (but see e.g. Pretzsch et al., 2014; Girardin et al., 2016). This approach is hampered by site-dependent effects and limited significance of these environmental conditions. A comprehensive understanding of tree functioning is urgently needed across broad regions in order to assess the potential and limits of forest carbon uptake globally (Chown, Gaston, & Robinson, 2004). Through the analysis of meaningful functional traits (Violle, Reich, Pacala, Enquist, & Kattge, 2014), the interpretation of spatiotemporal patterns of forest growth variability can provide comprehensive insights into the environmental responses that may change forest's services for carbon storage in the next decades (Anderegg et al., 2016).

The mechanisms and processes influencing forest growth are extremely variable (Gibert, Gray, Westoby, Wright, & Falster, 2016). Despite such complexity, regionally coherent multispecies responses have been linked to global change effects on forest ecosystems using tree-ring networks. For example, Babst et al. (2013) found well-defined biogeographic patterns in climate response of forest growth across Europe following latitudinal/elevational gradients, and Shestakova et al. (2016) reported a *ca*. 50% warming-induced enhanced growth synchrony in Iberian conifer forests during the 20th century. Indeed, dendroecological studies rely on the presence of common signals archived in tree populations, which are often derived from ring-width series reflecting variations of environmental factors (Fritts, 2001). Instead, stable isotopes are proxies of ecophysiological traits that are valuable to assess plant carbon and water relations at large spatiotemporal scales (Werner et al., 2012; Frank et al., 2015). Particularly, the ratio of the heavy to light carbon isotopes ($^{13}C/^{12}C$) of organic matter depends on factors controlling the plant's photosynthetic rate (A) and stomatal conductance (g_s) (Farquhar, Ehleringer, & Hubick, 1989). Since the carbon isotope discrimination ($\Delta^{13}C$) of tree rings reflect more directly the complex array of tree responses to the environment than classical traits such as ring-width (Treydte et al., 2007; Gessler et al., 2014), the interannual variation in tree-ring $\Delta^{13}C$ is often used to retrospectively recover information on leaf-level physiological processes (e.g., Berninger, Sonninen, Aalto, &

Lloyd, 2000; Andreu-Hayles et al., 2011; Shestakova, Aguilera, Ferrio, Gutiérrez, & Voltas, 2014). This is especially relevant in temperate forests thriving under near-optimal conditions, where tree growth fluctuations may not be as sensitive to climate factors as stable isotopes (Hartl-Meier et al., 2015). Indeed, additional information can be gained by analysing carbon isotopes in comparison to ring-widths (Cernusak & English, 2015). Both proxies provide evidence on how trees respond to climate change and increasing $_{atm}CO_2$ (Andreu-Hayles et al., 2011; Saurer et al., 2014).

In drought-prone environments, tree-ring $\Delta^{13}C$ can be mainly related to the stomatal control of CO_2 fluxes, integrating environmental conditions affecting stomatal conductance (Gessler et al., 2014). Under such conditions, radial growth (sink activity) and $\Delta^{13}C$ (source activity) are linked by two primary factors, stomatal regulation and water availability, with the feedback of sink activity on source activity being signaled through the phloem (Körner, 2015). However, radial growth and $\Delta^{13}C$ are progressively affected by changes in irradiance, temperature or nutritional stresses when water becomes less limited (Livingston et al., 1998; Rossi et al. 2016). By combining ring-width and $\Delta^{13}C$, information on tree performance can be gained that underlies biogeographical interactions, as such traits share spatial responses to drought events (Voelker, Meinzer, Lachenbruch, Brooks, & Guyette, 2014).

In the present study, we attempt to investigate the degree of association between stem growth and photosynthetic carbon isotope fractionation across European forests using a unique tree-ring network. So far, only the isotope data of this network have been analysed (Treydte et al., 2007), but not radial growth, nor their relationships. In this regard, Treydte et al. (2007) reported strong similarities in the response of carbon and oxygen isotope records to summer moisture conditions, suggesting a tight link at the leaf level mediated through variation in stomatal conductance caused by the combined effect of varying temperature and precipitation conditions (Scheidegger et al. 2000). We used 20 chronologies assembled from old trees comprising conifers (mainly *Pinus*) and oaks (*Quercus*) spanning the 20th century and ranging from Mediterranean to Boreal latitudes (37°N to 69°N). Indeed, latitudinal gradients are extremely relevant for the analysis of large-scale patterns of trait variability and their relationships with ecosystem functioning (Violle et al., 2014). We hypothesise that, on a continental scale, (i) temperature exerts – as a consequence of its large spatial homogeneity – a greater influence than drought on the spatial signals imprinted in tree rings; (ii) the relationship between ring-width and $\Delta^{13}C$ reflects the relative significance of carbon assimilation and stomatal regulation on tree performance, with positive relationships reflecting photosynthesis limited by stomatal conductance at low- and mid-latitude sites, and

negative relationships suggesting temperature- or light-limited carbon uptake at high-latitude sites; and (iii) widespread warming-induced drought stress triggers a tighter stomatal control of water loss that strengthens the relationship between growth and $\Delta^{13}C$ at low- and mid-latitude sites, as the stomatal sensitivity to drought becomes more limiting for carbon uptake. Therefore, we predict more synchronous growth linked to coordinated stomatal responses across species and regions as the climate becomes warmer and drier along the latitudinal gradient. On the basis of the combined analysis of radial growth and $\Delta^{13}C$, the assessment of spatiotemporal tree responses to environmental changes may improve our knowledge of growth and physiology changes experienced by European forests throughout the 20th century.

Materials and methods

Tree-ring network

We used a tree-ring dataset from the pan-European network ISONET (European Union, EVK2-2001-00237). It comprises 23 sites and provides a comprehensive coverage of the biogeographic conditions that are found across Europe into northern Africa (Treydte et al., 2007). The sites consist of old-growth forests (mean age = 454 ± 196 years [SD]) from the two main genera in Europe (*Pinus* and *Quercus*) plus *Cedrus atlantica* (Morocco) (Table 1). Three sites were discarded from the original network because they were located over 1,000 km apart from the nearest site (one site in southern Italy) or because they could not be properly assigned to a climate type consistent with that of nearby sites (two sites from high-elevation forests of the Alps) (for details, see subsection on *Analysis of spatiotemporal patterns in tree-ring signals*). The forests extend from cool dry-summer (Mediterranean basin) to humid temperate (western-central Europe), cold continental (north-central Europe) and subarctic (Fennoscandia) climates (Table 1, Fig. 1). The sampled trees are temperate oaks (*Quercus petraea* [3 sites], *Q. robur* [5 sites]) and Euro-Siberian pines (*Pinus nigra* [2 sites], *P. sylvestris* [8 sites], *P. uncinata* [1 site]) plus *Cedrus atlantica* (1 site), which has its phylogenetic origin in northern Eurasia (Qiao et al., 2007). Sampled stands show broad latitudinal (from 32°58'N to 68°56'N) and altitudinal (from 5 m to 2,100 m a.s.l.) gradients. High-elevation sites are concentrated in southern Europe. Mean annual temperature varies between –1.2°C and 11.5°C among sites, with January being the coldest month (range –14.1 to 5.1°C) and July the warmest month (11.9 to 19.6°C). Mean annual precipitation is highly variable, ranging from 432 mm to 1,517 mm across sites (Climatic Research Unit, CRU TS 3.21; Harris, Jones, Osborn, & Lister, 2014). Water deficit (i.e., evapotranspiration exceeding

precipitation) occurs for one month up to seven months (from March to October) depending on the geographic location (Table 1). Conifers are the dominant species in Boreal and Mediterranean zones (i.e., high-latitude or high-elevation sites), whereas oaks are mainly found in humid western and central European lowlands. The distance between sites varies from about 50 km up to 4,500 km.

Ring-width and carbon isotope information

Increment cores were extracted from dominant trees (site mean = 46 trees; median = 28) (Table S1), and tree-ring width (TRW) series were produced and cross-dated at the site level following standard dendrochronological procedures (Cook & Kairiukstis, 1990). TRW was measured under a binocular microscope with precision of 0.01 mm. Visual cross-dating and ring-width measurements were validated using the program COFECHA (Holmes, 1983). Individual series were then subjected to detrending with the Friedman supersmoother spline with variable span tweeter sensitivity α=5 (Friedman, 1984) and posterior autoregressive modelling. This procedure aims at eliminating biological growth trends and potential disturbance effects and generates stationary series of dimensionless residual indices (TRW_i) that preserve a common interannual variance (i.e., high-frequency variability potentially related to climate). Finally, site chronologies (20) were obtained by averaging the indexed values of the series using a bi-weight robust mean (Cook & Kairiukstis, 1990). These procedures were performed using the program ARSTAN (Cook & Krusic, 2013). The quality of the resulting site chronologies was evaluated by calculation of the mean inter-series correlation (*Rbar*) and the Expressed Population Signal (*EPS*) statistics. An *EPS* value of 0.85 was used to evaluate adequacy of the sample size for capturing a trustworthy population signal (Wigley, Briffa, & Jones, 1984). All chronologies were found to be well replicated during the 20th century (Table S1).

At least two accurately dated intact cores with clear ring boundaries and absence of missing rings from four or more trees per site were selected for subsequent carbon isotope analyses. Detailed information on sample preparation and α-cellulose extraction can be found in Treydte et al. (2007). In general, the whole ring was analysed for conifers, whereas only latewood was used for oaks. Treydte et al. (2007) reported that the type and magnitude of climate signals recorded in the isotopic network did not show obvious species-specific differences. To account for changes in $\delta^{13}C$ of atmospheric CO_2 ($\delta^{13}C_{air}$) due to fossil fuel combustion, carbon isotope discrimination ($\Delta^{13}C$) was estimated from $\delta^{13}C_{air}$ and α-cellulose $\delta^{13}C$ in plant material ($\delta^{13}C$), as described by Farquhar et al. (1989). Indexed $\Delta^{13}C$

chronologies ($\Delta^{13}C_i$) were obtained following the same procedure as described for ring-width. Hence, any physiological long-term trend (e.g., decadal-scale variability driven by potential changes in the response of trees to increased CO_2; McCarroll et al., [2009], Treydte et al., [2009]) was assumed to be removed from the series. In this way, we focused on the physiological basis of growth responses to high-frequency climate variability. TRW_i and $\Delta^{13}C_i$ chronologies were used as input for statistical analyses. The study period was 1901–2003.

Additionally, basal area increment (BAI) was calculated as a proxy for above-ground woody biomass accumulation. For this purpose, individual ring-width series were converted into BAI records and detrended using the Regional Curve Standardisation (RCS) method (Briffa and Melvin, 2011). This approach aimed at eliminating age/size effects but preserving long-term growth changes driven by environmental conditions (Peters et al., 2015). Next, the residual indices of BAI series were averaged at the site level using a bi-weight robust mean. Temporal trends in the resultant BAI chronologies were estimated through the slope of the linear regression of BAI records over the 20th century, and significant trends were determined using the non-parametric Kendall τ rank correlation coefficient (Table S1).

Meteorological data

Monthly mean temperature, precipitation and potential evapotranspiration were used for climate characterization. Meteorological variables were obtained from the nearest grid point of each site of the high-resolution climate dataset (Climatic Research Unit, CRU TS 3.21; Harris, Jones, Osborn, & Lister, 2014). CRU provides climate series on a 0.5° × 0.5° grid-box basis, interpolated from meteorological stations across the globe, and extends back to 1901. However, it should be noted that climate data mainly originate from low-elevation stations, and this leads to remarkable differences in elevation between stations and sampling sites in mountainous Mediterranean areas. To account for this discrepancy, we applied lapse rate adjustments to the CRU dataset for the Mediterranean sites (<45°N) following Gandullo (1994). Potential evapotranspiration was estimated from CRU records using the Hargreaves method (Hargreaves & Samani, 1982).

Bootstrapped correlations between TRW_i or $\Delta^{13}C_i$ chronologies and monthly temperature, precipitation and the Standardized Precipitation-Evapotranspiration Index (SPEI3, a 3-month integrated drought index integrating evaporative demand and water availability; Vicente-Serrano, Beguería, & López-Moreno, 2010) were computed over the period 1901–2003 to examine site-specific responses to climate. We used SPEI3 because

June-August is the period of highest climate responsiveness across the network for both TRW_i and, especially, $\Delta^{13}C_i$. To ensure that results were driven by local climate rather than by long-term trends (e.g., global warming), the climatic series exhibiting a linear trend over time were detrended by fitting a straight line and keeping the residuals of these linear fits or, otherwise, they were simply differenced from the grand mean. Climate relationships were analysed from the previous October to the current September of tree-ring formation.

Analysis of spatiotemporal patterns of tree-ring traits: methodological steps

The following steps were applied to characterise the nature and strength of common tree-ring patterns present in the network: first, we described the spatial structure of indexed tree-ring traits (TRW_i, $\Delta^{13}C_i$) across Europe through correlogram analyses; second, we investigated the temporal coherence of TRW_i among chronologies of the same or different climate type (i.e., within- and between-group respectively) through variance-covariance modelling; finally, we quantified the relationships between TRW_i and $\Delta^{13}C_i$ at the group level through a bivariate random model.

Characterization of the spatial structure of tree-ring traits across Europe

The spatial structure of tree-ring traits was characterized for site-pairs to determine how far common tree-ring patterns extend over Europe: This was done independently for TRW_i and $\Delta^{13}C_i$ as follows: (i) correlation coefficients (r) calculated between all possible pairs of site chronologies, calculated over the period 1901–2003, were regressed on their geographic distance using a negative exponential function; (ii) the statistical significance of these pairwise correlations was assessed within distance classes located 500 km apart – a compromise between number of classes and statistical power – using the modified correlogram technique (Koenig & Knops, 1998). Following (ii), six classes were defined ranging from <500 to >2,500 km, with chronologies farther than 2,500 km apart combined into a single class. The same analyses were performed for mean annual temperature and annual precipitation in order to evaluate the geographic extent of temporal coherence in such factors.

Temporal coherence of tree-ring width

The investigation of TRW_i variability among chronologies (growth synchrony, $\hat{a}$) was performed through variance-covariance (VCOV) modelling following Shestakova et al. (2014, 2018) (Appendix 1.1). This approach tests for the presence of different tree-ring

patterns for pre-established groups of chronologies, where particular groups can be defined based on existing knowledge (Shestakova et al., 2018). Here, the 20 chronologies were divided into four groups, i.e., classified according to particular climate types following the Köppen climate classification (Köppen & Geiger, 1936): Boreal (*Dfc*), cold continental (*Dfb*), humid temperate (C*fb*) and Mediterranean (*Csb*) (Table 1). Additionally, the humid temperate climate sites were split into Atlantic (for western Europe chronologies) and temperate (for central Europe chronologies) groups. These two groups resulted from a restriction of the maximum distance among sites belonging to the same group to 1,000 km (i.e., the spatial range of common tree-ring patterns continent-wide as inferred from correlograms). Therefore, five different groups were defined. Each group consisted of 3-5 neighbouring forest stands that ensured a solution to mixed model estimates.

A number of variance-covariance (VCOV) models accommodating between- and within-group variability were evaluated and compared using Akaike and Bayesian information criteria for model selection, which favour parsimonious models (Burnham & Anderson, 2002). The VCOV models were broad evaluation (constant variance across groups denoting a common growth pattern, or common synchrony, continent-wide), narrow evaluation (a banded main diagonal matrix denoting no common pattern or perfect asynchrony between groups), unstructured (a completely general covariance matrix indicating lack of systematic common patterns in the network), compound symmetry (a matrix having constant variance and covariance designating the same within-group pattern and the same between-group pattern) and variants of a Toeplitz structure (a matrix allowing for different (co)variances – denoting different patterns or synchrony values– according to the ordinal proximity or neighbourhood among groups). These models are described in detail in Table S2. Estimates of growth synchrony ($\hat{a}$) were derived using the best VCOV model for the entire period (1901–2003) (Shestakova et al., 2018). In addition, the evolution of changes in $\hat{a}$ was studied for successive 50-year segments (i.e., half the study period) lagged five years by fitting the same VCOV models to each segment. This was done to characterise shifts in common TRW_i variability over time. In this case, the best fitting model was independently selected for each segment to allow for changes in data structure over time.

Relationships between TRW_i and $\Delta^{13}C_i$ at the group level

The temporal (yearly) relation between TRW_i and $\Delta^{13}C_i$ (hereafter, r_Y) was investigated at the group level through a bivariate random-effects model (Appendix 1.2) (Shestakova et al., 2017). Broadly speaking, this approach estimates the extent by which TRW_i and $\Delta^{13}C_i$,

determined for the same set of chronologies, contain overlapping information as a result of plant processes related to carbon uptake and water use. Hence, the relevance of a physiological trait ($\Delta^{13}C_i$) potentially linked to regional forest growth is quantified by estimating how much of TRW_i variability across chronologies is associated with the variability of isotopic records. This quantification is relevant for studying the variable role of a physiological tracer for productivity across large areas. The bivariate analysis was performed for the entire period (1901–2003). We also evaluated the changes in r_Y between TRW_i and $\Delta^{13}C_i$ chronologies for successive 50-year segments lagged five years.

Finally, the changes in growth synchrony ($\hat{a}$) and in the relationship between TRW_i and $\Delta^{13}C_i$ (r_Y) were evaluated across groups as a function of biophysical variables through simple correlations. We used geographic information (latitude, longitude and elevation) and the following climatic records averaged across sites for every group (period 1901–2003): mean annual temperature (MAT), mean annual precipitation (MAP) and potential evapotranspiration (PET) following Hargreaves and Samani (1982). These relationships were assessed through correlation analysis for the complete period 1901–2003 and the split 1901–1950 and 1951–2003 periods.

Results

Absolute growth trends and climate responses of indexed chronologies

Five sites showed positive BAI trends (slope b, $P < 0.05$) for the period 1901–2003, while no significant trend was detected for the remaining sites (Table 1). Particularly, growth acceleration was observed at two oak sites and at three pine sites from mid and high latitudes of continental Europe. The analysis of climate responses revealed that high summer temperatures increased TRW_i in Fennoscandia principally (Fig. S1a). Conversely, drought stress often constrained TRW_i at central and southern latitudes as indicated by negative correlations with summer temperature and positive correlations with summer precipitation. Furthermore, strong ($r > 0.4$) positive correlations with SPEI3 that often extended from May to September denoted seasonal drought control of forest growth (Fig. S1a-c). In addition, the positive TRW_i responses to high winter temperatures observed at some mid- and low-latitude sites suggested co-limitation by cold winters and dry summers. In comparison, more clear-cut, strong ($|r| > 0.4$) climate signals were detected continent-wide for $\Delta^{13}C_i$ records, which were influenced by summer temperatures (negatively), summer precipitation (positively) and, especially, summer SPEI3 (positively) (Fig. S1d–f).

Spatial consistency of tree-ring signals

The correlations between pairs of chronologies for TRW_i decreased with increasing distance between sites. This effect accounted for 29% variability of inter-site correlation coefficients if subject to exponential decay (Fig. 2a). The highest correlations were found between *Quercus* stands from central Europe and between *Pinus* stands from north-eastern Europe ($r \geq 0.30$). For $\Delta^{13}C_i$, we also found an exponential decrease in common signal with distance for site-pairs, which accounted for 28% variability of inter-site correlation coefficients (Fig. 2b). Significant spatial autocorrelation was observed up to 1,000 km for TRW_i, with a mean correlation of 0.22 and 0.12 for sites within distances of 0–500 and 501–1,000 km, respectively (Fig. 2c). Spatial autocorrelation was also found for $\Delta^{13}C_i$ up to 1,000 km (Fig. 2d). A Principal Component Analysis performed on TRW_i returned five principal components (PCs) that accounted for 50% of the total variance. The first PC, which explained 12.9% of variance, had positive loadings for all chronologies, except for one Iberian site with *P. sylvestris* and the Moroccan site with *C. atlantica* (Fig. S2). The highest PC1 loadings corresponded to western and central European chronologies, indicating larger growth similarities compared to peripheral chronologies, located farther away from each other. The second PC, which explained 11.0% of variance, was also related to the geographic location of chronologies: positive PC2 loadings corresponded to south-western chronologies, while north-eastern chronologies had negative loadings (Fig. S2). The remaining three PCs accounted for <10% of variance and showed mixed spatial signals, indicating species-specific differences with the influence of local conditions on tree growth.

Similarly, the analysis of spatial autocorrelation of climate parameters revealed that the common signal declined with distance (Fig. S3a,b) and extended >2,500 km for MAT (linear function) and up to 1,000 km for MAP (decay function) (Fig. S3c,d). There was also a significant negative relation between the most distant sites (>2,500 km) for MAP.

Tree growth synchrony across Europe

The five climate groups identified for the network consisted of three to five chronologies sharing growth patterns (Fig. 1). A heterogeneous Toeplitz with two bands was the best VCOV model for the period 1901–2003, indicating covariation between neighbouring groups only (Table S3). Growth synchrony ($\hat{a}$) varied considerably across groups, ranging from 0.06 ± 0.01 (Mediterranean) to 0.36 ± 0.06 (Boreal) (mean ± SE) (Fig. 1). The $\hat{a}$ values were unrelated to the average distance between sites at the group level, with groups showing the lowest and highest $\hat{a}$ having inter-site distances of 785 ± 118 km and 913 ± 119 km

(mean ± SE), respectively. The variable number of chronologies at the group level neither influenced $\hat{a}$. At the between-group level, the highest $\hat{a}$ was found between Boreal and cold continental forests (0.11 ± 0.02), with progressively decreasing common signals between group neighbours observed southwards (Fig. 1). Differences in synchrony among groups were geographically structured and related to latitude ($r = 0.96$, $P < 0.01$) and longitude ($r = 0.89$, $P < 0.05$), but not to elevation (Fig. S4).

To check for geographic consistency of synchrony gradients across Europe, we examined an independent, larger set of ring-width chronologies obtained from the International Tree-Ring Data Bank (Grissino-Mayer & Fritts, 1997) having the same species representation ($n = 80$; 52 *Pinus* chronologies and 28 *Quercus* chronologies). In this case, we also detected a strong latitudinal gradient in $\hat{a}$ ($r = 0.83$, $P < 0.05$). Consequently, we assumed that this trend was essentially independent of the particular tree-ring network examined. The observed geographic gradient in growth synchrony was also analysed in relation to the potential climatic drivers of forest performance across Europe. Notably, climate variables explained most of the geographic variation in $\hat{a}$ among the five groups: strong negative relationships between $\hat{a}$ and PET ($r = -0.96$, $P < 0.01$), MAP ($r = -0.92$, $P < 0.05$) and MAT ($r = -0.81$, $P < 0.10$) were consistent with a gradual decrease in evapotranspirative demand, temperature and (elevation-driven) precipitation with increasing latitude.

Temporal changes in growth synchrony

The synchrony patterns changed markedly across Europe over the 20th century. $\hat{a}$ increased at low and mid latitudes (i.e., in Atlantic, Mediterranean and temperate forests), whereas it decreased at high latitudes (especially in Boreal, but also in cold continental forests) (Fig. 3a). Such divergent geographic trends modified the relation between $\hat{a}$ and biogeographic factors, resulting in geographically gentler $\hat{a}$ gradients across the continent after 1950 (Fig. S4). At the between-group level, different trends were observed depending on the particular group combination. For neighbouring groups, we found a substantial decrease in synchrony between Boreal and cold continental forests, whereas synchrony remained steady or increased for other group combinations (Fig. 3b). A modest, albeit sizeable common signal emerged among the more geographically distant group pairs after 1960 ($\hat{a} \approx 0.05$–0.10) (Fig. 3c). In fact, synchrony among forest types converged across Europe in the second half of the century. In contrast, we did not find changes in synchrony patterns of climate parameters (MAT, MAP) throughout the 20th century (results not shown). Therefore, the observed changes in growth

synchrony could not have been driven by concomitant fluctuations in synchrony of climate factors.

Tree growth patterns as related to isotopic signals

The temporal variability shared by TRW_i and $\Delta^{13}C_i$ (r_Y) was investigated at the group level. We found very different, geographically-structured relationships. The association was mainly positive (for Atlantic, cold-continental and temperate forests) or very positive (for Mediterranean forests), being significantly negative for Boreal forests (Fig. 1), hence following a latitudinal gradient ($r = -0.96$, $P < 0.01$). Conversely, r_Y was non-significant for neither longitude nor elevation. In addition, r_Y was correlated with climate variables at the group level, with the strongest positive association found for both PET ($r = 0.94$, $P < 0.05$) and MAP ($r = 0.82$, $P < 0.10$). An analysis across climate types involving all site chronologies of *Quercus* spp. confirmed that the positive relationship observed in Central Europe was taxa-independent ($r_Y = 0.32$, SE=0.21).

The association between TRW_i and $\Delta^{13}C_i$ changed markedly across Europe throughout the 20th century (Fig. 4). r_Y turned from negative to non-significant in Boreal forests, and changed from non-significant to positive in cold-continental (recently), temperate and Mediterranean forests. As a result, TRW_i and $\Delta^{13}C_i$ mainly became positively related across Europe. The latitudinal pattern of r_Y was also stronger in the second half ($r = -0.95$, $P < 0.05$) than in the first half of the century ($r = -0.58$, n.s.). This relationship became more dependent on PET after 1950 ($r = 0.95$, $P < 0.05$) than before 1950 ($r = 0.68$, n.s.).

Discussion

This study yields evidence for geographically-structured patterns of forest growth and its associations with carbon isotope fractionation processes across Europe. Common tree growth and physiology are shared by stands being up to 1,000 km apart from each other. This outcome provides the geographical extent up to which climate factors influence tree performance continent-wide; indeed, no other environmental driver is likely to act on the same spatial scale at the high-frequency domain (Fritts, 2001).

Geographic structure of climatic controls of tree-ring signals in European forests

Differential growth responses to climate were evident across the network, with temperature-sensitive growth at northern latitudes, precipitation-sensitive growth at central-southern latitudes, and mixed signals in temperate and high-elevation European

forests (Babst et al., 2013). Conversely, the extent of common summer climate signals present in carbon isotopes suggests a tight stomatal control of water losses and, indirectly, photosynthetic activity at peak season across most of Europe (Cullen, Adams, Anderson, & Grierson, 2008). These results suggest a partial de-coupling between leaf- and stem-level processes (Jucker et al., 2017) as the result of different potentially contributing processes: (i) environmental constraints governing sink activity (i.e. meristematic growth) before affecting source activity (i.e., carbon uptake), particularly under drought or low temperatures (Körner et al. 2015), (ii) temporal shifts between foliar dynamics and xylogenesis (Seftigen et al. 2018), and (iii) changes in carbon allocation patterns with increasing temperature which may vary between different biomes and functional groups (Way & Oren, 2010).

Interpreting ring-width patterns continent-wide

Our results show a marked geographical organization of 20th-century growth patterns across Europe. The most conspicuous changes in synchronous tree growth occur along a north–south gradient, with *â* increasing northwards concurrent with a thermal gradient of decreasing temperature and reduced evapotranspiration. This agrees with our hypothesis of more synchronous growth in cold-limited, high-latitude forests owing to the greater spatial homogeneity of temperature effects on tree growth in northern Europe (Düthorn, Schneider, Günther, Gläser, & Esper, 2016). This is in contrast with the geographically complex drought events occurring in central and southern Europe (Orlowsky & Seneviratne, 2014), hence resulting in substantially less synchronous growth occurring at large spatial scales (Shestakova et al., 2016). It should be noted that the mixture of sites with different species (oaks or pines) at the mid-latitude climate types may have intrinsically reduced the magnitude of synchronous growth in central Europe. Similarly, the inclusion of a cedar chronology may have constrained synchrony at the southernmost (Mediterranean) group, although *Cedrus atlantica* has a stomatal behaviour similar to *P. nigra* (Froux et al. 2002). Species-specific climate responses are indeed relevant to delineate valid biogeographic patterns of tree performance, as shown Europe-wide (Babst et al. 2013). Perhaps due to the limited density of our network we could not clearly identify such differences (Fig. S1), but the investigation of a denser dataset with nearly the same species representation confirmed such a broad latitudinal gradient (Fig. S5). Thus, the results of a common sampling effort of limited representativeness compare well with records compiled from miscellaneous investigations having particular goals, geographic scopes and sampling strategies.

Notably, *â* increased after 1950 except in Fennoscandia, hence weakening the northward trend of enhanced synchrony observed during the preceding period. It suggests warming-induced climatic forcing spreading across central and southern Europe, irrespective of species and local site conditions (Fig. S6). This exogenous factor enhances synchrony likely as the outcome of common tree sensitivity to increased water stress. The results are in line with previous findings of high-frequency adjustments of ring-width patterns in response to amplified drought effects on growth in temperate and semiarid regions (Latte, Lebourgeois, & Claessens, 2015; Shestakova et al., 2016). In contrast, climate warming could progressively mitigate low-temperature constraints on tree performance occurring in Boreal forests (Düthorn et al., 2016). This leads to an increasing importance of local (stand-level) effects on tree growth over time, hence triggering regional asynchrony (Shestakova et al., 2019). We interpret these phenomena as a sign of increasing drought impacts on forest growth dynamics expanding northwards across Europe, which are concurrent with temperature trends across the study area (+0.15 to +0.35°C/decade between 1960 and 2015) (EEA, 2016).

Carbon isotope fractionation points to spatial patterns of forest growth in Europe

We also investigated leaf-level physiological mechanisms linked to geographically-structured temporal growth variability by modelling the common temporal signal present in TRW_i and $\Delta^{13}C_i$ through bivariate random-effects analysis. This approach is appropriate for investigating common constraints on forest growth and leaf physiology acting over large (continental) climate gradients, because site-level impacts on tree-ring traits (e.g., differential management, competition, soil depth and fertility, etc.) are explicitly set aside in the analysis.

For the entire study period, the positive relationship between TRW_i and $\Delta^{13}C_i$ at low and mid latitudes indicates that leaf-level physiology and tree growth are commonly driven by water stress, to a greater or lesser extent, south of ≈60°N in Europe (Fig. 1). Therefore, it suggests that stomatal limitation of carbon assimilation is imprinted in tree growth at most of the study area (including e.g., France, Austria, Germany and Poland) during the 20th century. This observation is seemingly independent of differences in stomatal behaviour between oaks and pines (Roman et al. 2015). Regardless of the different amplitude of $\Delta^{13}C$ fluctuations determined by isohydric and anisohydric strategies, the observed high-frequency signals share similar characteristics across taxa, as already reported by Treydte et al. (2007). Conversely, the negative relationship between TRW_i and $\Delta^{13}C_i$ in Fennoscandia indicates that photosynthesis and, also, meristematic activity are constrained by low temperatures/sunshine hours (Gagen et al., 2011). At cool, moist sites the main control over water-use efficiency is

assimilation rate, which can be limited by either enzyme activity (photon flux) or enzyme production (leaf temperature or nitrogen availability). These limitations would increase $\Delta^{13}C$ at the expense of decreased carbon uptake, which may reduce radial growth. Undoubtedly, our results must be weighed against the limited spatial density of the sampling network, but they allow delineating broad geographical trends that so far have been difficult to ascertain continent-wide, partly due to the unsystematic and sparse nature of data collection (Saurer et al., 2014). Besides, the observed trends agree with previous studies performed across smaller areas showing strong positive TRW_i *vs.* $\Delta^{13}C$ correlations for trees growing under water-limited conditions, but weak correlations at wetter and colder sites (Voelker et al., 2014; del Castillo, Voltas, & Ferrio, 2015).

Strengthening of $\Delta^{13}C$–growth relationships in response to climate change

The relation between tree growth and carbon isotope fractionation was not stable during the 20th century, with a general tendency towards increasing $\Delta^{13}C$–growth coupling across Europe. Alongside the increase in growth synchrony observed in the Atlantic, temperate and Mediterranean groups, a change from non-significant to positive correlations across most continental Europe suggests intensified drought impacts on tree physiology since the 1970s. Remarkably, present-day climatic influences on continent-wide tree growth are predominantly related to water conservation strategies, as reflected in cellulose $\Delta^{13}C$. In this regard, we found evidence of growth enhancement in the network (positive BAI trends), but only in five high- and mid-latitude stands (over 50°N) composed of either *Quercus* spp. or *P. sylvestris*. In these sites, the increasing trend could be produced by a raise in photosynthetic rates or in meristematic activity, which are likely driven by a combination of rising CO_2, temperature and surface radiation. On the other hand, drought stress seems to override a positive effect of enhanced leaf intercellular CO_2 concentration in the remaining sites, and particularly below 50°N (e.g., the Mediterranean group, where the relation TRW_i *vs.* $\Delta^{13}C$ became strongly positive since 1970), resulting in no change in productivity (Andreu-Hayles et al., 2011). However, such warming-induced drought effects influencing stomatal regulation are insufficient to provoke the 20th-century Europe-wide decrease of forest transpiration, as demonstrated for the same network (Frank et al., 2015). Alternative factors (e.g., lengthened growing seasons or increased leaf area) may counterbalance the impacts of leaf-level gas exchange processes on whole-tree physiology (Frank et al., 2015).

In Fennoscandia, the negative ring-width dependence on $\Delta^{13}C$ vanished after 1950. This suggests that an earlier photosynthetic limitation of growth or, alternatively, a reduced

meristematic activity determining low carbon uptake – as driven by low temperatures, high cloudiness or both factors – attenuated in recent decades. In the western Mediterranean, this dependence changed abruptly from zero to nearly one after 1970. Previously, growth synchrony among the Mediterranean chronologies was absent, rendering a null signal shared by ring-width and $\Delta^{13}C$. After 1950, the common growth signal was low but relevant: this signal was essentially related to $\Delta^{13}C$ fluctuations, resulting in a highly positive correlation (albeit with a high SE; Fig. 1). This correlation may be interpreted in terms of a tight stomatal control of common radial growth in high-mountain Mediterranean forests, but it could also imply drought-driven reductions of sink activity controlling photosynthesis (Muller et al. 2011). However, the limited number of chronologies and the sudden change in tree performance during the 20th century might question these interpretations. A recent study carried out in Iberian mountain forests allows the downscaling of our results to a local area (Shestakova et al., 2017). These authors reported that multispecies tree growth at about 1,500 m is more associated with a tighter stomatal control of water losses (inferred from $\Delta^{13}C$) since the 1980s, hence resembling lower elevation stands. These results reinforce our view, although more data supporting this evidence are still needed on a regional scale. Unfortunately, studies on long-term shifts of radial growth related to switches of the main environmental drivers of photosynthetic carbon gain are still scarce (Voelker et al., 2014).

To conclude, we report on a shift in forest growth dependence from low temperatures to low moisture occurring southwards continent-wide and associated with latitudinal changes of tree carbon isotope fractionation processes. Leaf-level physiology and radial growth of trees are ultimately linked via carbon allocation strategies. Common signals imprinted in ring-width and stable isotopes have been reported, either along geographical gradients (i.e., phenotypic plasticity; del Castillo et al., 2015), over time (i.e., temporal covariation; Voelker et al., 2014; Shestakova et al., 2017; this work) or at the intraspecific level (i.e., genetic correlation; Fardusi et al., 2016). These evidences support (direct or indirect) effects of carbon uptake processes on above-ground growth. On the other hand, carbohydrates are used for various other processes than growth (e.g., maintenance, respiration, reproduction) and carbon availability might seldom limit tree growth (Palacio, Hoch, Sala, Körner, & Millard, 2014; but see Wiley & Helliker, 2012), which suggests that the relationship between productivity and stable isotopes may not be straightforward (Jucker et al., 2017). Alternative physiological mechanisms related to above-ground growth may interact with photosynthetic processes; for example, a critical turgor disrupting cell growth or the appearance of hydraulic constraints under drought (Sperry, 2000), or the weakening of meristematic growth under low

temperatures (Rossi et al., 2016). These mechanisms would need to be carefully assessed against stable isotope signals.

Together with climate change, the increasing $_{atm}CO_2$ may have played a role in the observed shift in growth synchrony and the stronger relation between $\Delta^{13}C$ and TRW_i. Disentangling the relative effects of climate and CO_2 fertilization on spatially structured tree-ring information is challenging because both low- and high-frequency signals influence the behaviour of tree physiology, carbon allocation and above- and below-ground growth. Additional factors interacting with climate change and $_{atm}CO_2$ such as increasing nutrient limitations (Jonard et al., 2015) or atmospheric deposition (de Vries, Dobbertin, Solberg, van Dobben, & Schaub, 2014) should also be considered. A previous study on the same tree-ring network demonstrated that CO_2 fertilization has increased water-use efficiency of European forests in the 20th century (Saurer et al., 2014). However, these increments were not spatially uniform and, notably, the strongest increase was reported in response to summer drought for temperate forests in central Europe, an area in which we observe a large rise in growth-$\Delta^{13}C$ coupling. These findings point to increase of water stress spreading northwards across European forests. Therefore, broad-scale climatic variation influences tree ecophysiology and productivity in previously unrecognized ways, and points to coordinated shifts in forest growth dynamics and a progressive convergence in the response of trees to the new climate conditions across Europe.

References

Anderegg, W. R. L., Klein, T., Barlett, M., Sack, L., Pellegrini, A. F., Choat, B., & Jansen, S. (2016). Meta-analysis reveals that hydraulic traits explain cross-species patterns of drought-induced tree mortality across the globe. *Proceedings of the National Academy of Sciences of the United States of America*, **113**, 5024–5029.

Andreu-Hayles, L., Gutiérrez, E., Muntan, E., Helle, G., Anchukaitis, K. J., & Schleser, G. H. (2011). Long tree-ring chronologies reveal 20th century increases in water-use efficiency but no enhancement of tree growth at five Iberian pine forests. *Global Change Biology*, **17**, 2095–2112.

Babst, F., Poulter, B., Trouet, V., Tan, K., Neuwirth, B., Wilson, R., Carrer, M., Grabner, M., Tegel, W., Levanič, T., Panayotov, M., Urbinati, C., Bouriaud, O., Ciais, P., & Frank, D. (2013). Site- and species-specific responses of forest growth to climate across the European continent. *Global Ecology and Biogeography*, **22**, 706–717.

Berninger F., Sonninen E., Aalto T., & Lloyd J. (2000). Modeling ^{13}C discrimination in tree rings. *Global Biogeochemical Cycles*, **14**, 213–223.

Briffa, K. R., & Melvin, T. M. (2011). A closer look at Regional Curve Standardization of tree-ring records: Justification of the need, a warning of some pitfalls, and suggested improvements of its application. In: Hughes, M. K., Diaz, H. F., Swetnam, T. W. (eds) Dendroclimatology: Progress and Prospects. Berlin: Springer Verlag, pp. 113–145.

Burnham, K. P., & Anderson, D. R. (2002) *Model selection and multi-model inference: A practical information – theoretic approach*. Springer, New York 488 pp.

Cernusak, L. A., & English, N. B. (2015). Beyond tree-ring widths: stable isotopes sharpen the focus of climate response of temperate forest trees. *Tree Physiology*, **35**, 1–3.

Chown, S. L., Gaston, K. J., & Robinson, D. (2004). Macrophysiology: large-scale patterns in physiological traits and their ecological implications. *Functional Ecology*, **18**, 159–167.

Cook, E. R., & Kairiukstis, L. A. (1990). *Methods of dendrochronology: Applications in the environmental sciences*. Dordrecht, Netherlands: Springer Netherlands.

Cook, E. R., & Krusic, P. J. (2013). *Program ARSTAN. A tree-ring standardization program based on detrending and autoregressive time series modeling, with interactive graphics*. Palisades, NY: Columbia University.

Cullen, L. E., Adams, M. A., Anderson, M. J., & Grierson, P. F. (2008). Analyses of $\delta^{13}C$ and $\delta^{18}O$ in tree rings of *Callitris columellaris* provide evidence of a change in stomatal

control of photosynthesis in response to regional changes in climate. *Tree Physiology*, **28**, 1525–1533.

de Vries, W., Dobbertin, M. H., Solberg, H., van Dobben, H. F., & Schaub, M. (2014). Impacts of acid deposition, ozone exposure and weather conditions on forest ecosystems in Europe: an overview. *Plant and Soil*, **380**, 1–45.

del Castillo, J., Voltas, J., & Ferrio, J. P. (2015). Carbon isotope discrimination, radial growth, and NDVI share spatiotemporal responses to precipitation in Aleppo pine. *Trees*, **29**, 223–233.

Düthorn, E., Schneider, L., Günther, B., Gläser, S., & Esper, J. (2016). Ecological and climatological signals in tree-ring width and density chronologies along a latitudinal boreal transect. *Scandinavian Journal of Forest Research*, **31**, 750–757.

European Environment Agency (2016). *Trends in annual temperature across Europe between 1960 and 2015*. [WWW document] URL http://www.eea.europa.eu/data-and-maps/figures/decadal-average-trends-in-mean-6. [accessed 1 August 2018].

Fardusi, M. S., Ferrio, J. P., Comas, C., Voltas, J., Resco de Dios, V., & Serrano, L. (2016). Intra-specific association between carbon isotope composition and productivity in woody plants: a meta-analysis. *Plant Science*, **251**, 110–118.

Farquhar, G. D., Ehleringer, J. R., & Hubick, K. T. (1989). Carbon isotope discrimination and photosynthesis. *Annual Review of Plant Physiology and Plant Molecular Biology*, **40**, 503–537.

Frank, D. C., Poulter, B., Saurer, M., Esper, J., Huntingford, C., Helle, G., Treydte, K., Zimmermann, N. E., Schleser, G. H., Ahlström, A., Ciais, P., Friedlingstein, P., Levis, S., Lomas, M., Sitch, S., Viovy, N., Andreu-Hayles, L., Bednarz, Z., Berninger, F., Boettger, T., D'Alessandro, C. M., Daux, V., Filot, M., Grabner, M., Gutierrez, E., Haupt, M., Hilasvuori, E., Jungner, H., Kalela-Brundin, M., Krapiec, M., Leuenberger, M., Loader, N. J., Marah, H., Masson-Delmotte, V., Pazdur, A., Pawelczyk, S., Pierre, M., Planells, O., Pukiene, R., Reynolds-Henne, C. E., Rinne, K. T., Saracino, A., Sonninen, E., Stievenard, M., Switsur, V. R., Szczepanek, M., Szychowska-Krapiec, E., Todaro, L., Waterhouse, J. S., & Weigl, M. (2015). Water-use efficiency and transpiration across European forests during the Anthropocene. *Nature Climate Change*, **5**, 579–584.

Friedman, J. H. (1984). *A variable span smoother*. Stanford, CA: Stanford University.

Fritts, H. C. (2001). *Tree rings and climate*. Caldwell, NJ: Blackburn Press.

Froux, F., Huc, R., Ducrey, M., Dreyer, E. (2002). Xylem hydraulic efficiency versus vulnerability in seedlings of four contrasting Mediterranean tree species (*Cedrus atlantica*, *Cupressus sempervirens*, *Pinus halepensis* and *Pinus nigra*). *Annals of Forest Science*, **59**, 409–418.

Gagen, M., Zorita, E., McCarroll, D., Young, G. H. F., Grudd, H., Jalkanen, R., Loader, N. J., Robertson, I., & Kirchhefer, A. (2011). Cloud response to summer temperatures in Fennoscandia over the last thousand years. *Geophysical Research Letters*, **38**, L05701.

Gandullo, J. M. (1994). *Climatología y ciencia del suelo*. Madrid, Spain: Fundación Conde del Valle de Salazar.

Gessler, A., Ferrio, J. P., Hommel, R., Treydte, K., Werner, R., & Monson, R. K. (2014). Stable isotopes in tree rings: toward a mechanistic understanding of fractionation and mixing processes from the leaves to the wood. *Tree Physiology*, **34**, 796–818.

Gibert, A., Gray, E. F., Westoby, M., Wright, I. J., & Falster, D. S. (2016). On the link between functional traits and growth rate: meta-analysis shows effects change with plant size, as predicted. *Journal of Ecology*, **104**, 1488–1503.

Girardin, M.P., Bouriaud, O., Hogg, E.H., Kurz, W., Zimmermann, N.E., Metsaranta, J.M., de Jong, R., Frank, D.C., Esper, J., Büntgen, U., Guo, X.J., Bhatti, J. (2016) No growth stimulation of Canada's boreal forest under half-century of combined warming and CO_2 fertilization. *Proceedings of the National Academy of Sciences of the United States of America*, **113**, E8406–E8414.

Grissino-Mayer, H. D, & Fritts, H. C. (1997). The International Tree-Ring Data Bank: an enhanced global database serving the global scientific community. *Holocene*, **7**, 235–228.

Hargreaves, G. H., & Samani, Z. A. (1982). Estimating potential evapotranspiration. *Journal of the Irrigation & Drainage Division – ASCE*, **108**, 225–230.

Harris, I., Jones, P. D., Osborn, T. J., & Lister, D. H. (2014). Updated high-resolution grids of monthly climatic observations – the CRU TS3.10 Dataset. *International Journal of Climatology*, **34**, 623–642.

Hartl-Meier, C., Zang, C., Büntgen, U., Esper, J., Rothe, A., Göttlein, A., Dirnböck, T., & Treydte, K. (2015). Uniform climate sensitivity in tree-ring stable isotopes across species and sites in a mid-latitude temperate forest. *Tree Physiology*, **35**, 4–15.

Holmes, R. L. (1983). Computer-assisted quality control in tree-ring dating and measurement. *Tree Ring Bulletin*, **43**, 69–78.

Jonard, M., Fürst, A., Verstraeten, A., Thimonier, A., Timmermann, V., Potočić, N., Waldner, P., Benham, S., Hansen, K., Merilä, P., Ponette, Q., de la Cruz, A. C., Roskams, P., Nicolas, M., Croisé, L., Ingerslev, M., Matteucci, G., Decinti, B., Bascietto, M., & Rautio, P. (2015). Tree mineral nutrition is deteriorating in Europe. *Global Change Biology*, **21**, 418–430.

Jucker, T., Grossiord, C., Bonal, D., Bouriaud, O., Gessler, A., & Coomes, D. A. (2017). Detecting the fingerprint of drought across Europe's forests: do carbon isotope ratios and stem growth rates tell similar stories? *Forest Ecosystems*, **4**, 24.

Koenig, W. D., & Knops, J. M. H. (1998). Testing for spatial autocorrelation in ecological studies. *Ecography*, **21**, 423–429.

Köppen, W., & Geiger, R. (1936). Handbuch der klimatologie. Berlin, Germany: Gebrüder Bornträger.

Körner, C. (2015). Paradigm shift in plant growth control. *Current Opinion in Plant Biology*, **25**, 107–114.

Latte, N., Lebourgeois, F., & Claessens, H. (2015). Increased tree-growth synchronization of beech (*Fagus sylvatica* L.) in response to climate change in northwestern Europe. *Dendrochronologia*, **33**, 69–77.

Livingston, N. J., Whitehead, D., Kelliher, F. M., Wang, Y. P., Grace, J. C., Walcroft, A. S., Byers, J. N., Mcseveny, T. M. & Millard, P. (1998) Nitrogen allocation and carbon isotope fractionation in relation to intercepted radiation and position in a young *Pinus radiata* D. Don tree. *Plant, Cell & Environment*, **21**, 795–803.

McCarroll, D., Gagen, M. H., Loader, N. J., Robertson, I., Anchukaitis, K. J., Los, S., Young, G. H. F, Jalkanen, R., Kirchhefer, A., & Waterhouse, J. S. (2009). Correction of tree ring stable carbon isotope chronologies for changes in the carbon dioxide content of the atmosphere. *Geochimica et Cosmochimica Acta*, **73**, 1539–1547.

Muller, B., Pantin, F., Genard, M., Turc, O., Freixes, S., Piques, M., & Gibon, Y. (2011). Water deficits uncouple growth from photosynthesis, increase C content, and modify the relationships between C and growth in sink organs. *Journal of Experimental Botany*, **62**, 1715–1729.

Nabuurs, G. J., Lindner, M., Verkerk, P. J., Gunia, K., Deda, P., Michalak, R., & Grassi, G. (2013). First signs of carbon sink saturation in European forest biomass. *Nature Climate Change*, **3**, 792–796.

Orlowsky, B., & Seneviratne, S. I. (2014). On the spatial representativeness of temporal dynamics at European weather stations. *International Journal of Climatology*, **34**, 3154–3160.

Palacio, S., Hoch, G., Sala, A., Körner, C., & Millard, P. (2014). Does carbon storage limit tree growth? *New Phytologist*, **201**, 1096–1100.

Peters, R. L., Groenendijk, P., Vlam, M., & Zuidema, P. A. (2015). Detecting long-term growth trends using tree rings: A critical evaluation of methods. *Global Change Biology*, **21**, 2040–2054.

Pretzsch, H., Biber, P., Schütze, G., Uhl, E., & Rötzer, T. (2014) Forest stand growth dynamics in Central Europe have accelerated since 1870. *Nature Communications*, **5**, 4967.

Roman, D. T., Novick, K. A., Brzostek, E. R., Dragoni, D., Rahman, F., & Phillips, R. P. (2015). The role of isohydric and anisohydric species in determining ecosystem-scale response to severe drought. *Oecologia*, **179**, 641–654.

Qiao, C-Y., Ran, J-H., Li, Y., & Wang, X-Q. (2007) Phylogeny and biogeography of *Cedrus* (Pinaceae) inferred from sequences of seven paternal chloroplast and maternal mitochondrial DNA regions. *Annals of Botany*, **100**, 573–580.

Rossi, S., Anfodillo, T., Čufar, K., Cuny, H. E., Deslauriers, A., Fonti, P., Frank, D., Gričar, J., Gruber, A., Huang, J. G., Jyske, T., Kašpar, J., King, G., Krause, C., Liang, E., Mäkinen, H., Morin, H., Nöjd, P., Oberhuber, W., Prislan, P., Rathgeber, C. B., Saracino, A., Swidrak, I., & Treml, V. (2016). Pattern of xylem phenology in conifers of cold forest ecosystems at the Northern Hemisphere. *Global Change Biology*, **22**, 3804–3813.

Saurer, M., Spahni, R., Frank, D. C., Joos, F., Leuenberger, M., Loader, N. J., McCarroll, D., Gagen, M., Poulter, B., Siegwolf, R. T. W., Andreu-Hayles, L., Boettger, T., Dorado Liñán, I., Fairchild, I. J., Friedrich, M., Gutiérrez, E., Haupt, M., Hilasvuori, E., Heinrich, I., Helle, G., Grudd, H., Jalkanen, R., Levanič, T., Linderholm, H. W., Robertson, I., Sonninen, E., Treydte, K., Waterhouse, J. S., Woodley, E. J., Wynn, P. M., & Young, G. H. (2014). Spatial variability and temporal trends in water-use efficiency of European forest. *Global Change Biology*, **20**, 332–336.

Scheidegger, Y., Saurer, M., Bahn, M., & Siegwolf, R. (2000). Linking stable oxygen and carbon isotopes with stomatal conductance and photosynthetic capacity: a conceptual model. *Oecologia*, **125**, 350–357.

Seftigen, K., Frank, D.C., Björklund, J., Babst, F., Poulter, B. (2018). The climatic drivers of normalized difference vegetation index and tree-ring-based estimates of forest productivity are spatially coherent but temporally decoupled in Northern Hemispheric forests. *Global Ecology and Biogeography*, **27**, 1352–1365.

Shestakova, T. A., Aguilera, M., Ferrio, J. P., Gutiérrez, E., & Voltas, J. (2014). Unravelling spatiotemporal tree-ring signals in Mediterranean oaks: a variance–covariance modelling approach of carbon and oxygen isotope ratios. *Tree Physiology*, **34**, 819–838.

Shestakova, T. A., Gutiérrez, E., Kirdyanov, A. V., Camarero, J. J., Génova, M., Knorre, A. A., Linares, J. C., Resco de Dios, V., Sánchez-Salguero, R., & Voltas, J. (2016). Forests synchronize their growth in contrasting Eurasian regions in response to climate warming. *Proceedings of the National Academy of Sciences of the United States of America*, **113**, 662–667.

Shestakova, T. A., Camarero, J. J., Ferrio, J. P., Knorre, A. A., Gutiérrez, E., & Voltas, J. (2017). Increasing drought effects on five European pines modulate Δ^{13}C-growth coupling along a Mediterranean altitudinal gradient. *Functional Ecology*, **31**, 1359–1370.

Shestakova, T. A., Gutiérrez, E., & Voltas, J. (2018). A roadmap to disentangling ecogeographical patterns of spatial synchrony in dendrosciences. *Trees*, **32**, 359–370.

Shestakova, T. A., Gutiérrez, E., Valeriano, C., Lapshina, E., & Voltas, J. (2019). Recent loss of sensitivity to summer temperature constrains tree growth synchrony among boreal Eurasian forests. *Agricultural and Forest Meteorology*, **268**, 318–330.

Sperry, J. S. (2000). Hydraulic constraints on plant gas exchange. *Agricultural and Forest Meteorology*, **104**, 13–23.

Treydte, K., Frank, D. C., Esper, J., Andreu, L., Bednarz, Z., Berninger, F., Boettger, T., D'Alessandro, C. M., Etien, N., Filot, M., Grabner, M., Guillemin, M. T., Gutierrez, E., Haupt, M., Helle, G., Hilasvuori, E., Jungner, H., Kalela-Brundin, M., Krapiec, M., Leuenberger, M., Loader, N. J., Masson-Delmotte, V., Pazdur, A., Pawelczyk, S., Pierre, M., Planells, O., Pukiene, R., Reynolds-Henne, C. E., Rinne, K. T., Saracino, A., Saurer, M., Sonninen, E., Stievenard, M., Switsur, V. R., Szczepanek, M., Szychowska-Krapiec, E., Todaro, L., Waterhouse, J. S., Weigl, M., & Schleser, G. H. (2007). Signal strength and climate calibration of a European tree-ring isotope network. *Geophysical Research Letters*, **34**, L24302.

Treydte, K., Frank, D. C., Saurer, M., Helle, G., Schleser, G. H., & Esper, J. (2009). Impact of climate and CO_2 on a millennium-long tree-ring carbon isotope record. *Geochimica et Cosmochimica Acta*, **73**, 4635–4647.

Vicente-Serrano, S. M., Beguería, S., & López-Moreno, J. I. (2010). A Multiscalar drought index sensitive to global warming: the Standardized Precipitation Evapotranspiration Index. *Journal of Climate*, **23**, 1696–1718.

Violle, C., Reich, P. B., Pacala, S. W., Enquist, B. J., & Kattge, J. (2014). The emergence and promise of functional biogeography. *Proceedings of the National Academy of Sciences of the United States of America*, **111**, 13690–13696.

Voelker, S. L., Meinzer, F. C., Lachenbruch, B., Brooks, J. R., & Guyette, R. P. (2014). Drivers of radial growth and carbon isotope discrimination of bur oak (*Quercus macrocarpa* Michx.) across continental gradients in precipitation, vapour pressure deficit and irradiance. *Plant, Cell and Environment*, **37**, 766–779.

Way, D. A., & Oren, R. (2010). Differential responses to changes in growth temperature between trees from different functional groups and biomes: a review and synthesis of data. *Tree Physiology*, **30**, 669–688.

Wigley, T. M. L., Briffa, K. R., & Jones, P. D. (1984). On the average value of correlated time series, with applications in dendroclimatology and hydrometerology. *Journal of Applied Meteorology and Climatology*, **23**, 201–213.

Werner, C., Schnyder, H., Cuntz, M., Keitel, C., Zeeman, M. J., Dawson, T. E., Badeck, F. W., Brugnoli, E., Ghashghaie, J., Grams, T. E. E., Kayler, Z. E., Lakatos, M., Lee, X., Maguas, C., Ogee, J., Rascher, K. G., Siegwolf, R. T. W., Unger, S., Welker, J., Wingate, L., & Gessler, A. (2012). Progress and challenges in using stable isotopes to trace plant carbon and water relations across scales. *Biogeosciences*, **9**, 3083–3111.

Wiley, E. & Helliker, B. (2012). A re-evaluation of carbon storage in trees lends greater support for carbon limitation to growth. *New Physiologist*, **195**, 285-289.

Data Accessibility Statement

The tree-ring data used in this study are available in the International Tree Ring Data Bank (ITRDB). The $\delta^{13}C$ records are available in Supporting Information of Treydte et al. (2007), grl23621-sup-0003-fs02.eps file.

FIGURE CAPTIONS

Figure 1. Geographical distribution of sites, definition of groups of chronologies, synchrony of radial growth ($\hat{a}$), and relationship between TRW_i and $\Delta^{13}C_i$ chronologies (r_Y) at the group level across Europe. Each dot identifies a chronology composed of $n \geq 20$ trees according to the codes shown in Table 1 (oak codes are shown in italics). Each coloured encircled area identifies a group of chronologies that are separated in pairs up to 1,000 km and belong to a particular climate type as indicated in Table 1 (see Fig. 2c for the distance threshold where significant radial growth patterns are shared among chronologies). At least three sites of the same climate type form a group (total number of groups, $n = 5$). $\hat{a}$ and r_Y values are estimated using indexed chronologies for the period 1901–2003 as described in Appendix 1.1 (Supporting Information). Growth synchrony ($\hat{a}$) is shown within a rectangle (at the within-group level) and within an ellipse (at the between-group level) respectively. Only chronologies belonging to pairs of groups that are geographically close (i.e. neighbour groups) have between-group synchrony values statistically different from zero for the entire study period (as shown in the figure). The correlations at the group level (r_Y) are tested directly in a bivariate mixed model using REML, and estimates are shown in the insets together with their standard error (SE). The scatterplots show year-level estimates (BLUPs) of TRW_i and $\Delta^{13}C_i$ extracted from the bivariate model. Significant correlations (those having confidence intervals which not straddle zero, 90% CI approximated as $r_Y \pm 1.64SE$) are indicated with lines. The high SEs are partly explained by the errors of BLUP predictions that are carried forward in the bivariate analyses.

Figure 2. Spatial patterns of indexed tree-ring traits across Europe for the period 1901–2003: **(a, c)** indexed tree-ring width (TRW_i), **(b, d)** indexed carbon isotope discrimination ($\Delta^{13}C_i$). *(Left panels)* Pairwise correlations of tree-ring chronologies as a function of geographical distance. The patterns are summarised by regressing the correlation coefficients (r values) involving pairs of chronologies (y-axis) on their corresponding distance (x-axis) by using negative exponential functions. Dot colours indicate pairwise correlations involving two conifer chronologies (green), two oak chronologies (orange), and one conifer and oak chronology (blue). Asterisks after the correlation coefficient (r_M) indicate the level of significance based on a Mantel test ($^{***}P < 0.001$). *(Right panels)* Spatial structure of tree-ring traits across European forests. The spatial autocorrelation of the tree-ring network was characterized by six consecutive distance classes (listed on the x-axis). Mean r values and

their statistical significance (P) within each distance class were estimated from 1,000 randomizations. Significant correlation coefficients ($P < 0.05$) are indicated by an asterisk.

Figure 3. Temporal trends in growth synchrony at within- and between-group levels for the period 1901–2003. Growth synchrony ($\hat{a}$) is estimated for 50-year periods lagged by 5 years following Eqs. 5 and 6 as described in Appendix 1.1 (Supporting Information). All calculations are based on indexed ring-width (TRW_i) chronologies. For the sake of visual clarity, the estimates of $\hat{a}$ are represented separately for chronologies belonging to the same group (i.e., within-group level) **(a)**, for chronologies belonging to pairs of groups that are geographically close (i.e. neighbour groups) **(b)**, and for chronologies belonging to pairs of groups that are geographically distant **(c)**. Grey lines denote the SE. Note the change in scale of the Y-axis between panels.

Figure 4. Temporal trends of relations between TRW_i and $\Delta^{13}C_i$ chronologies at the group level for the period 1901–2003. The correlations (r_Y) are estimated for 50-year periods lagged five years following Eq. 7 as described in Appendix 1.2 (Supporting Information). All calculations are based on indexed ring-width (TRW_i) and carbon isotope ($\Delta^{13}C_i$) chronologies. Grey lines denote the SE of r_Y. Significant correlations (correlation coefficients with 90% confidence intervals not embracing zero) are depicted by filled dots.

Table 1. Geographical features and climatic characteristics of the sampling sites. Sites are sorted latitudinally, from north (top) to south (bottom). Climate parameters were obtained based on CRU TS 3.21 data over the period 1901–2003 (see Materials and Methods for details). Climate types were estimated using the Köppen classification (Köppen & Geiger, 1936).

No	Country	Site name	Code	Species	Latitude (°N)	Longitude (°E)	Elevation (m)	MAT (°C)	MAP (mm)	PET (mm)	MAP < PET	BAI trend, *b* ($cm^2\ yr^{-1}$)	Köppen classification
1	Finland	Kessi, Inari	INA	*Pinus sylvestris*	68.93	28.42	150	–1.2	432	413	Apr-Aug	0.038	Dfc, subarctic
2	Finland	Sivak., Ilomantsi	ILO	*Pinus sylvestris*	62.98	31.27	200	2.2	573	515	Apr-Aug	0.152*	Dfc, subarctic
3	Norway	Gutuli	GUT	*Pinus sylvestris*	62.00	12.18	800	0.7	586	512	Apr-Aug	0.115	Dfc, subarctic
4	Finland	Bromarv	BRO	*Quercus robur*	60.00	23.08	5	4.9	568	562	Apr-Aug	0.004	Dfb, cold continental
5	UK	Lochwood	LOC	*Quercus robur*	55.27	–3.43	175	7.4	1517	589	Jun	–0.032	Cfb, humid temperate
6	Lithuania	Panemunes Silas	PAN	*Pinus sylvestris*	54.88	23.97	45	6.6	634	672	Apr-Sep	0.320***	Dfb, cold continental
7	Poland	Suwalki	SUW	*Pinus sylvestris*	54.10	22.93	160	6.7	619	686	Apr-Sep	–0.010	Dfb, cold continental
8	UK	Woburn Abbey	WOB	*Quercus robur*	51.98	–0.59	50	9.5	709	724	Apr-Sep	0.046	Cfb, humid temperate
9	Germany	Dransfeld	DRA	*Quercus petraea*	51.50	9.78	320	7.7	723	677	Apr-Sep	0.163*	Cfb, humid temperate
10	UK	Windsor	WIN	*Pinus sylvestris*	51.41	–0.59	10	9.5	763	738	Apr-Sep	0.102	Cfb, humid temperate
11	Poland	Niepolomice, Gibiel	NIE1	*Quercus robur*	50.12	20.38	190	8.0	676	674	Apr-Aug	0.156*	Dfb, cold continental
12	Poland	Niepolomice, Gibiel	NIE2	*Pinus sylvestris*	50.12	20.38	190	8.0	676	674	Apr-Aug	0.250***	Dfb, cold continental
13	France	Fontainebleau	FON	*Quercus petraea*	48.38	2.67	100	11.5	608	861	Mar-Sep	–0.129	Cfb, humid temperate
14	France	Rennes	REN	*Quercus robur*	48.25	–1.70	100	11.1	733	786	Apr-Sep	–0.064	Cfb, humid temperate
15	Austria	Lainzer Tiergarte	LAI	*Quercus petraea*	48.18	16.20	300	9.6	654	792	Mar-Sep	–0.024	Cfb, humid temperate
16	Austria	Poellau	POE	*Pinus nigra*	47.95	16.06	500	8.3	815	762	Apr-Aug	–0.053	Cfb, humid temperate
17	Spain	Pinar de Lillo	LIL	*Pinus sylvestris*	43.07	–5.25	1600	5.1	1505	688	Jul-Aug	0.069	Csb, Mediterranean
18	Spain	Massis de Pedraforca	PED	*Pinus uncinata*	42.23	1.70	2100	3.9	1299	692	Jul-Aug	–0.052	Csb, Mediterranean
19	Spain	Sierra de Cazorla	CAZ	*Pinus nigra*	37.80	–2.95	1816	8.9	712	1014	May-Sep	0.022	Csb, Mediterranean
20	Morocco	Col du Zad	COL	*Cedrus atlantica*	32.97	–5.07	2200	10.4	717	1163	Apr-Oct	–0.055	Csb, Mediterranean

Abbreviations: MAT, mean annual temperature; MAP, mean annual precipitation; PET, potential evapotranspiration; BAI, basal area increment

*$P < 0.05$; **$P < 0.01$; ***$P < 0.001$. The significance of BAI trends is assessed using the Kendall's τ non-parametric rank correlation coefficient.

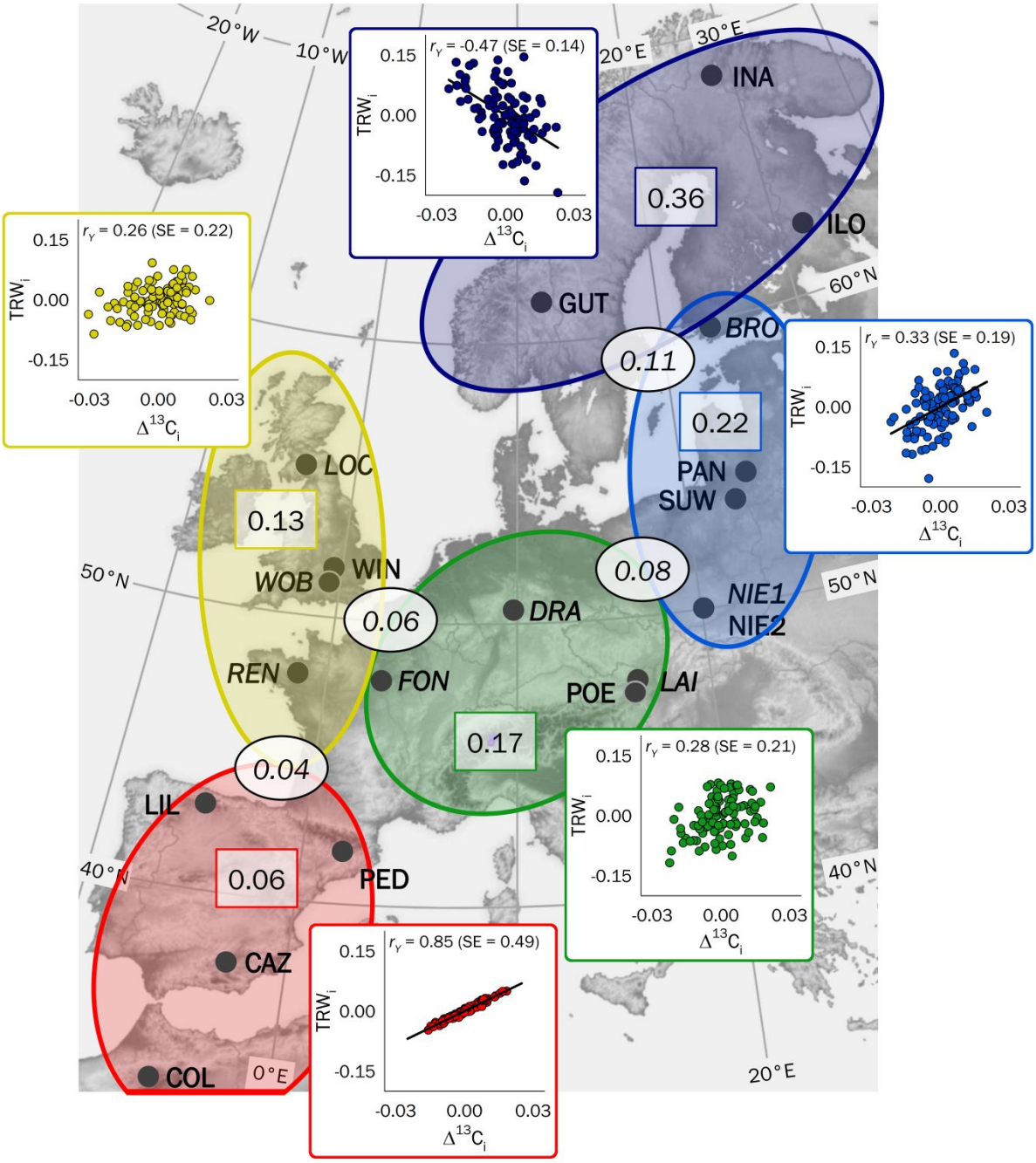
20°W
10°W
20°E
30°E
60°N
50°N
40°N
0°E
20°E
INA
ILO
GUT
BRO
LOC
WOB
WIN
DRA
NIE1
NIE2
PAN
SUW
REN
FON
POE
LAI
LIL
PED
CAZ
COL
0.36
0.11
0.22
0.13
0.08
0.06
0.17
0.04
0.06
r_Y = -0.47 (SE = 0.14)
r_Y = 0.26 (SE = 0.22)
r_Y = 0.33 (SE = 0.19)
r_Y = 0.28 (SE = 0.21)
r_Y = 0.85 (SE = 0.49)
TRW$_i$
$\Delta^{13}C_i$
0.15
0.00
-0.15
-0.03
0.03

Figure 1

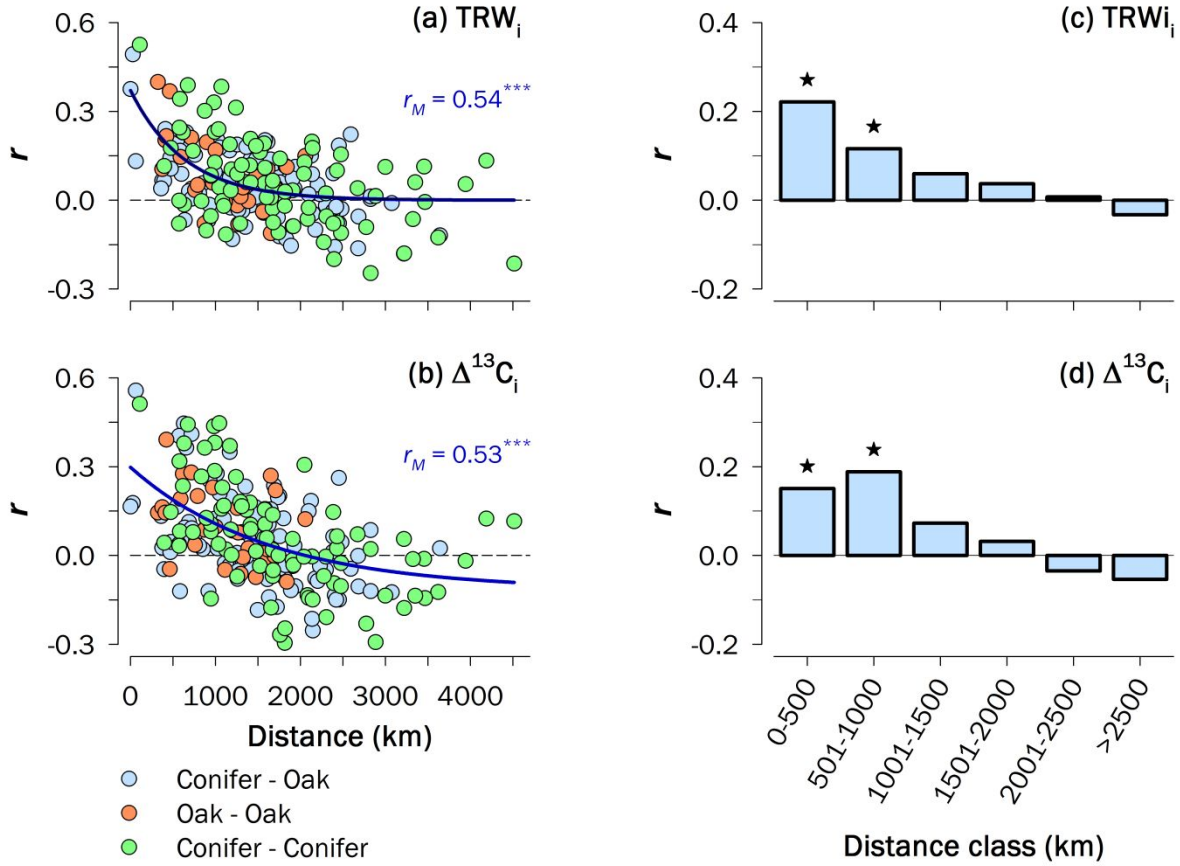

Figure 2

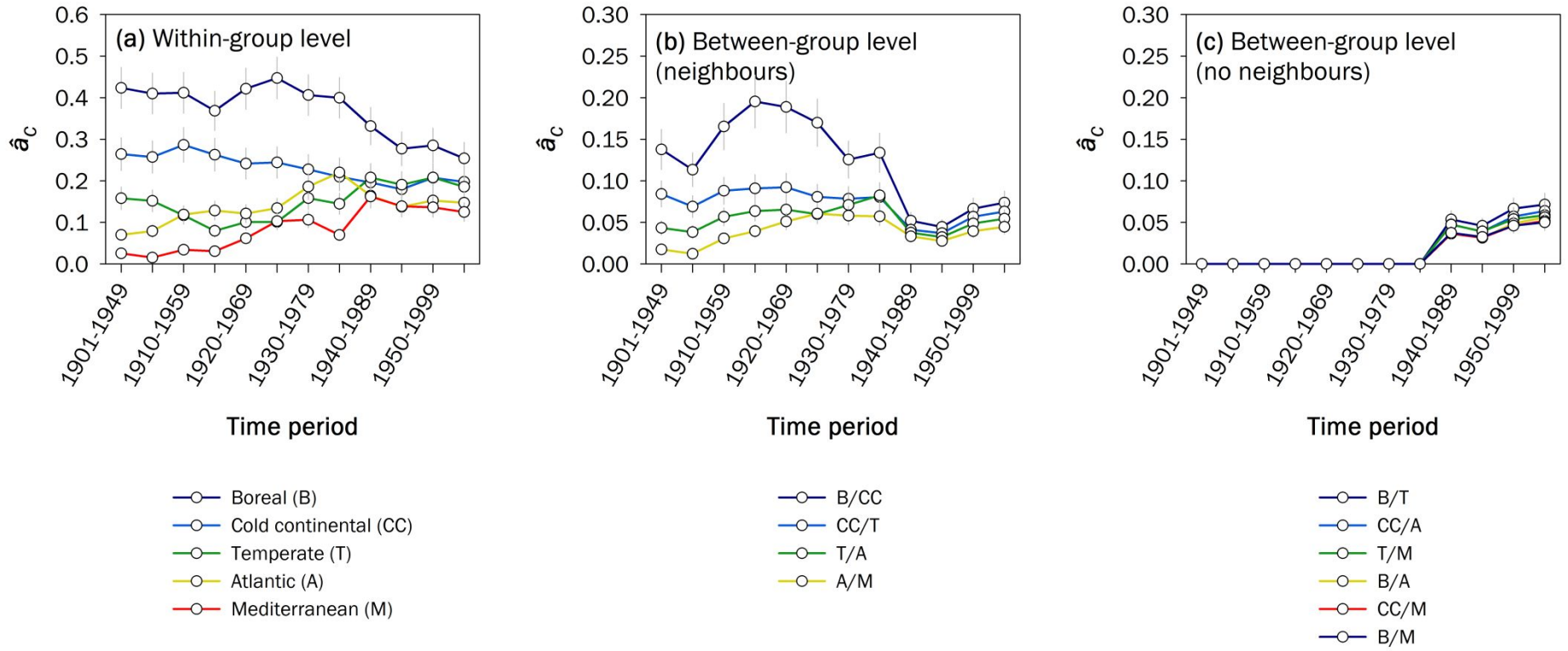

871

872 **Figure 3**

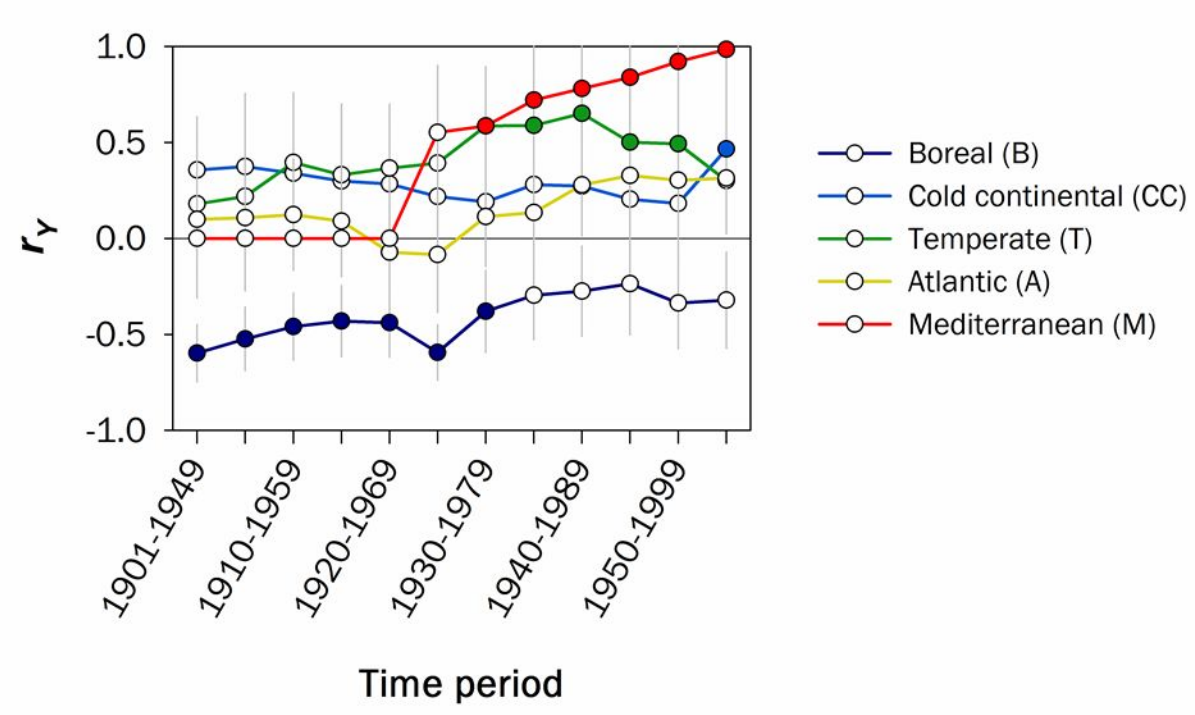

Figure 4

Supporting Information

Additional Supporting Information may be found in the online version of this article:

Appendix 1. Mixed modelling analysis.

Table S1. Dendrochronological characteristics of the study sites.

Table S2. Description of variance-covariance (VCOV) models accommodating between- and within-group variability.

Table S3. Results of variance-covariance models for synchrony analysis.

Figure S1. Climate signals at the site level for TRW_i and $\Delta^{13}C_i$ for the period 1901–2003.

Figure S2. Principal component analysis performed on 20 indexed ring-width chronologies distributed across Europe and northern Africa for the common period 1901–1998.

Figure S3. Spatial patterns of climate signals (mean annual temperature, MAT; mean annual precipitation, MAP) across Europe for the period 1901–2003.

Figure S4. Geographical patterns of growth synchrony ($\hat{a}$) at the group level for the entire period 1901–2003 and change in $\hat{a}$ for two consecutive periods (1901–1950 and 1951–2003).

Figure S5. Geographical patterns of growth synchrony ($\hat{a}$) for chronologies obtained from the International Tree-Ring Data Bank (ITRDB) dataset for the period 1901–2003.

Figure S6. Trends in climate parameters: mean annual temperature (MAT) and mean annual precipitation (MAP) at the group level.

SUPPORTING INFORMATION

Supplementary Text

Appendix 1. Random modelling analysis

1.1. Temporal coherence of ring-width signals among chronologies

The investigation of common ring-width fluctuations among chronologies (i.e., common signal strength) was performed through mixed modelling as described in Shestakova et al. (2014). Let W_{ij} stand for TRW_i of the *i*th chronology in the *j*th year. Then the estimators can be defined in terms of the following random model:

$$W_{ij} = Y_j + e_{ij} \quad (2)$$

where Y_j is a random effect of the *j*th year and e_{ij} is a random deviation of the *i*th chronology in the *j*th year. Here, we assume that the year effects behave as if they came from a normal distribution with mean zero and variance σ_Y^2. We also assume that random effects from different random terms (Y_j and e_{ij}) are independent of each other (Demidenko, 2004). The reproducibility of observations by the set of *I* chronologies (i = 1 to n) can be estimated as (Shestakova et al., 2014):

$$\hat{a} = \frac{\sigma_Y^2}{\sigma_Y^2 + \sigma_e^2} \quad (3)$$

We refer to $\hat{a}$ as the intra-class correlation or growth synchrony among chronologies. Intra-class correlation close to 1 indicates near-perfect synchrony among chronologies, while a value close to 0 denotes spatial asynchrony.

If we hypothesize about the presence of different sources of similarities–dissimilarities among tree-ring records (e.g., pertinence to a particular climate type), then model (2) can be expanded to an alternative mixed model by adding a fixed effect β_r (r = 1 to m). In this case, the estimators can be defined as follows:

$$W_{ijr} = \beta_r + Y_{jr} + e_{ijr} \quad (4)$$

where β_r is a fixed term accounting for mean differences among the m groups, Y_{jr} is the random effect of the j^{th} year in the r^{th} group, and e_{ijr} is the residual term (i.e., a random deviation of the i^{th} chronology in the j^{th} year within the r^{th} group).

To analyse temporal patterns in synchrony within and between groups with distinct growth signals, corresponding to the five climate types (r = 1 to 5; see Materials and Methods

section for details), the following variance-covariance (VCOV) structure underlying model (2) was initially employed (Shestakova et al., 2014):

$\text{cov}(\underline{Y}_{jr};\underline{Y}_{jr^*}) = \sigma^2_{Y_r}$, when $r = r^*$,

otherwise $\text{cov}(\underline{Y}_{jr};\underline{Y}_{jr^*}) = \sigma^2_{Y_{rr^*}}$

This general VCOV structure (or unstructured model) allows each group to have its own year variance and each pair of groups its own year covariance. The mean correlation (synchrony) estimated between all possible pairs of chronologies as in Eq. 2 can be split into (i) a mean correlation between pairs of chronologies within every group r and (ii) a mean correlation between pairs of chronologies belonging to groups r and r^*, as follows (Shestakova et al., 2014):

$$\hat{a}_{Cw} = \frac{\sigma^2_{Y_r}}{\sigma^2_{Y_r} + \sigma^2_e} \quad (5)$$

$$\hat{a}_{Cb} = \frac{\sigma^2_{Y_{rr^*}}}{\sqrt{(\sigma^2_{Y_r} + \sigma^2_e) \times (\sigma^2_{Y_{r^*}} + \sigma^2_e)}} \quad (6)$$

Mixed models allow for flexible modelling of complex intra- and inter-group correlation patterns and heteroscedastic errors, hence providing estimates to solve Eqs. (5) and (6). Alternative, more parsimonious variance–covariance (VCOV) structures than the general (unstructured) VCOV structure also used to model tree-ring signals are provided in Table S2.

1.2. Relationships between radial growth and stable isotopes

The temporal associations between traits (TRW_i, $\Delta^{13}C_i$) were investigated at the group level through bivariate analyses (Holland, 2006). Following Shestakova et al. (2017), the single trait random model (2) was extended to take into account simultaneously the information available on a pair of traits (TRW_i and $\Delta^{13}C_i$) as follows: the temporal (yearly) component of a Pearson correlation between traits (which also includes residual cross-product effects) was estimated by partitioning the general covariance (i.e., across years and chronologies) into its year and residual components. In particular, the correlation of year effects (r_Y) was calculated as:

$$r_Y = \frac{\sigma_{Y_{12}}}{\sqrt{\sigma^2_{Y_1} \times \sigma^2_{Y_2}}} \quad (7)$$

where $\sigma_{Y_{12}}$ is the common variability (covariance) of year effects underlying traits 1 and 2, $\sigma^2_{Y_1}$ stands for the variance of year effects for trait 1 and $\sigma^2_{Y_2}$ stands for the variance of year effects for trait 2.

The statistical analyses were performed with SAS/STAT (ver. 9.4, SAS Inc., Cary, NC, USA). We used the MIXED procedure for variance-covariance modelling and estimation of variance components through restricted maximum likelihood (REML). Specifically, combined variance-covariance estimation of two traits by multivariate REML analysis was implemented through the RANDOM statement using a full (or unstructured) variance-covariance matrix (Holland, 2006).

Supplementary References

Demidenko, E. (2004). *Mixed models: theory and applications*. New York, NY: John Wiley & Sons.

Grissino-Mayer, H. D., & Fritts, H. C. (1997). The International Tree-Ring Data Bank: an enhanced global database serving the global scientific community. *Holocene*, **7**, 235–228.

Holland, J. B. (2006). Estimating genotypic correlations and their standard errors using multivariate restricted maximum likelihood estimation with SAS Proc MIXED. *Crop Science*, **46**, 642–654.

Shestakova, T. A., Aguilera, M., Ferrio, J. P., Gutiérrez, E., & Voltas, J. (2014). Unravelling spatiotemporal tree-ring signals in Mediterranean oaks: a variance–covariance modelling approach of carbon and oxygen isotope ratios. *Tree Physiology*, **34**, 819–838.

Shestakova, T. A., Camarero, J. J., Ferrio, J. P., Knorre, A. A., Gutiérrez, E., & Voltas, J. (2017). Increasing drought effects on five European pines modulate Δ^{13}C-growth coupling along a Mediterranean altitudinal gradient. *Functional Ecology*, **31**, 1359–1370.

Shestakova, T. A., Gutiérrez, E., & Voltas, J. (2018). A roadmap to disentangling ecogeographical patterns of spatial synchrony in dendrosciences. *Trees*, **32**, 359–370.

Supplementary Tables

Table S1. Dendrochronological characteristics of the sampling sites. Mean values are calculated over the period 1901–2003. Abbreviations: *EPS*, Expressed Population Signal; *Rbar*, mean interseries correlation; TRW, tree-ring width; $\Delta^{13}C$, carbon isotope discrimination. The variability of mean values is expressed as standard deviation (SD).

No	Code	Species	No. trees/cores	Time span	*EPS* > 0.85 since	*Rbar*±SD	TRW±SD (mm)	$\Delta^{13}C$±SD (‰)
1	Ina	*Pinus sylvestris*	15/32	1508–2003	1570	0.44±0.10	0.52±0.15	18.46±0.44
2	Ilo	*Pinus sylvestris*	28/39	1580–2003	1610	0.33±0.07	0.29±0.04	17.81±0.40
3	Gut	*Pinus sylvestris*	45/89	1449–2004	1510	0.45±0.10	0.50±0.08	17.39±0.54
4	Bro	*Quercus robur*	7/19	1822–2004	1850	0.44±0.13	1.84±0.60	18.90±0.74
5	Loc	*Quercus robur*	28/38	1706–2003	1750	0.29±0.14	1.16±0.25	19.30±0.58
6	Pan	*Pinus sylvestris*	30/61	1487–2003	1590	0.28±0.11	0.79±0.21	16.93±0.54
7	Suw	*Pinus sylvestris*	76/76	1600–2004	1620	0.31±0.14	1.02±0.28	17.10±0.80
8	Wob	*Quercus robur*	20/30	1613–2003	1640	0.44±0.11	1.37±0.24	17.37±0.91
9	Dra	*Quercus petraea*	16/45	1770–2002	1800	0.49±0.11	1.42±0.49	17.53±0.68
10	Win	*Pinus sylvestris*	16/21	1763–2003	1790	0.28±0.12	1.22±0.31	16.90±0.62
11	Nie1	*Quercus robur*	35/39	1768–2003	1810	0.37±0.11	1.88±0.40	19.83±0.91
12	Nie2	*Pinus sylvestris*	72/78	1622–2003	1650	0.25±0.15	1.01±0.32	17.36±0.98
13	Fon	*Quercus petraea*	30/60	1306–2000	1530	0.31±0.13	0.87±0.31	17.85±0.72
14	Ren	*Quercus robur*	11/30	1751–1998	1860	0.43±0.17	1.63±0.53	18.89±0.45
15	Lai	*Quercus petraea*	55/81	1462–2003	1510	0.39±0.17	1.18±0.18	18.86±0.71
16	Poe	*Pinus nigra*	326/588	1319–2002	1500	0.37±0.11	0.62±0.18	18.32±0.60
17	Lil	*Pinus sylvestris*	15/32	1511–2002	1560	0.35±0.10	0.47±0.12	16.22±0.55
18	Ped	*Pinus uncinata*	23/56	1269–2003	1510	0.33±0.09	0.49±0.10	15.91±0.51
19	Caz	*Pinus nigra*	33/68	1125–2002	1190	0.47±0.10	0.47±0.09	15.03±0.41
20	Col	*Cedrus atlantica*	10/40	1560–2000	1590	0.51±0.09	1.12±0.26	14.50±0.42

Table S2. Description of variance-covariance (VCOV) models accommodating between- and within-group variability (adapted from Shestakova et al. [2014] and Shestakova et al. [2018]). The models constrain different elements of the year × group (G) variance-covariance structure. The residual (R) variance-covariance structure is a diagonal matrix with constant (homogeneous residuals, HR) or non-constant (heterogeneous residuals, HeR) terms. The number of parameters to be estimated is shown for each model (#par).

Hypothesis testing	G matrix	R matrix – HR	R matrix – HeR	#par (HR / HeR)
Broad evaluation. Null model ignoring groups	σ^2	σ_ε^2	–	2 / –
Narrow evaluation. Lack of common signal between groups	$\begin{pmatrix} \sigma_1^2 & 0 & 0 & 0 & 0 \\ 0 & \sigma_2^2 & 0 & 0 & 0 \\ 0 & 0 & \sigma_3^2 & 0 & 0 \\ 0 & 0 & 0 & \sigma_4^2 & 0 \\ 0 & 0 & 0 & 0 & \sigma_5^2 \end{pmatrix}$	σ_ε^2	$\begin{pmatrix} \sigma_{\varepsilon_1}^2 & 0 & 0 & 0 & 0 \\ 0 & \sigma_{\varepsilon_2}^2 & 0 & 0 & 0 \\ 0 & 0 & \sigma_{\varepsilon_3}^2 & 0 & 0 \\ 0 & 0 & 0 & \sigma_{\varepsilon_4}^2 & 0 \\ 0 & 0 & 0 & 0 & \sigma_{\varepsilon_5}^2 \end{pmatrix}$	6 / 20
Compound symmetry. Constant variance and covariance	$\begin{pmatrix} \sigma^2+\sigma_1 & \sigma_1 & \sigma_1 & \sigma_1 & \sigma_1 \\ \sigma_1 & \sigma^2+\sigma_1 & \sigma_1 & \sigma_1 & \sigma_1 \\ \sigma_1 & \sigma_1 & \sigma^2+\sigma_1 & \sigma_1 & \sigma_1 \\ \sigma_1 & \sigma_1 & \sigma_1 & \sigma^2+\sigma_1 & \sigma_1 \\ \sigma_1 & \sigma_1 & \sigma_1 & \sigma_1 & \sigma^2+\sigma_1 \end{pmatrix}$	σ_ε^2	$\begin{pmatrix} \sigma_{\varepsilon_1}^2 & 0 & 0 & 0 & 0 \\ 0 & \sigma_{\varepsilon_2}^2 & 0 & 0 & 0 \\ 0 & 0 & \sigma_{\varepsilon_3}^2 & 0 & 0 \\ 0 & 0 & 0 & \sigma_{\varepsilon_4}^2 & 0 \\ 0 & 0 & 0 & 0 & \sigma_{\varepsilon_5}^2 \end{pmatrix}$	3 / 7
Heterogeneous Toeplitz. Different variances and covariances for all group pairs depending on their ordinal geographic proximity	$\begin{pmatrix} \sigma_1^2 & \sigma_1\sigma_2\rho_1 & \sigma_1\sigma_3\rho_2 & \sigma_1\sigma_4\rho_3 & \sigma_1\sigma_5\rho_4 \\ \sigma_1\sigma_2\rho_1 & \sigma_2^2 & \sigma_2\sigma_3\rho_1 & \sigma_2\sigma_4\rho_2 & \sigma_2\sigma_5\rho_3 \\ \sigma_1\sigma_3\rho_2 & \sigma_2\sigma_3\rho_1 & \sigma_3^2 & \sigma_3\sigma_4\rho_1 & \sigma_3\sigma_5\rho_2 \\ \sigma_1\sigma_4\rho_3 & \sigma_2\sigma_4\rho_2 & \sigma_3\sigma_4\rho_1 & \sigma_4^2 & \sigma_4\sigma_5\rho_1 \\ \sigma_1\sigma_5\rho_4 & \sigma_2\sigma_5\rho_3 & \sigma_3\sigma_5\rho_2 & \sigma_4\sigma_5\rho_1 & \sigma_5^2 \end{pmatrix}$	σ_ε^2	$\begin{pmatrix} \sigma_{\varepsilon_1}^2 & 0 & 0 & 0 & 0 \\ 0 & \sigma_{\varepsilon_2}^2 & 0 & 0 & 0 \\ 0 & 0 & \sigma_{\varepsilon_3}^2 & 0 & 0 \\ 0 & 0 & 0 & \sigma_{\varepsilon_4}^2 & 0 \\ 0 & 0 & 0 & 0 & \sigma_{\varepsilon_5}^2 \end{pmatrix}$	10 / 14

Heterog. Toeplitz with two bands. Different variances and (co)variances for geographically contiguous group pairs only	$\begin{pmatrix} \sigma_1^2 & \sigma_1\sigma_2\rho_1 & 0 & 0 & 0 \\ \sigma_1\sigma_2\rho_1 & \sigma_2^2 & \sigma_2\sigma_3\rho_1 & 0 & 0 \\ 0 & \sigma_2\sigma_3\rho_1 & \sigma_3^2 & \sigma_3\sigma_4\rho_1 & 0 \\ 0 & 0 & \sigma_3\sigma_4\rho_1 & \sigma_4^2 & \sigma_4\sigma_5\rho_1 \\ 0 & 0 & 0 & \sigma_4\sigma_5\rho_1 & \sigma_5^2 \end{pmatrix}$	σ_ε^2	$\begin{pmatrix} \sigma_{\varepsilon_1}^2 & 0 & 0 & 0 & 0 \\ 0 & \sigma_{\varepsilon_2}^2 & 0 & 0 & 0 \\ 0 & 0 & \sigma_{\varepsilon_3}^2 & 0 & 0 \\ 0 & 0 & 0 & \sigma_{\varepsilon_4}^2 & 0 \\ 0 & 0 & 0 & 0 & \sigma_{\varepsilon_5}^2 \end{pmatrix}$	7 / 11
Heterog. Toeplitz with three bands. Different variances and (co)variances for geographically contiguous group pairs of first and second order.	$\begin{pmatrix} \sigma_1^2 & \sigma_1\sigma_2\rho_1 & \sigma_1\sigma_3\rho_2 & 0 & 0 \\ \sigma_1\sigma_2\rho_1 & \sigma_2^2 & \sigma_2\sigma_3\rho_1 & \sigma_2\sigma_4\rho_2 & 0 \\ \sigma_1\sigma_3\rho_2 & \sigma_2\sigma_3\rho_1 & \sigma_3^2 & \sigma_3\sigma_4\rho_1 & \sigma_3\sigma_5\rho_2 \\ 0 & \sigma_2\sigma_4\rho_2 & \sigma_3\sigma_4\rho_1 & \sigma_4^2 & \sigma_4\sigma_5\rho_1 \\ 0 & 0 & \sigma_3\sigma_5\rho_2 & \sigma_4\sigma_5\rho_1 & \sigma_5^2 \end{pmatrix}$	σ_ε^2	$\begin{pmatrix} \sigma_{\varepsilon_1}^2 & 0 & 0 & 0 & 0 \\ 0 & \sigma_{\varepsilon_2}^2 & 0 & 0 & 0 \\ 0 & 0 & \sigma_{\varepsilon_3}^2 & 0 & 0 \\ 0 & 0 & 0 & \sigma_{\varepsilon_4}^2 & 0 \\ 0 & 0 & 0 & 0 & \sigma_{\varepsilon_5}^2 \end{pmatrix}$	8 / 12
Unstructured. Completely general covariance matrix	$\begin{pmatrix} \sigma_1^2 & \sigma_{12} & \sigma_{13} & \sigma_{14} & \sigma_{15} \\ \sigma_{12} & \sigma_2^2 & \sigma_{23} & \sigma_{24} & \sigma_{25} \\ \sigma_{13} & \sigma_{23} & \sigma_3^2 & \sigma_{34} & \sigma_{35} \\ \sigma_{14} & \sigma_{24} & \sigma_{34} & \sigma_4^2 & \sigma_{45} \\ \sigma_{15} & \sigma_{25} & \sigma_{35} & \sigma_{45} & \sigma_5^2 \end{pmatrix}$	σ_ε^2	$\begin{pmatrix} \sigma_{\varepsilon_1}^2 & 0 & 0 & 0 & 0 \\ 0 & \sigma_{\varepsilon_2}^2 & 0 & 0 & 0 \\ 0 & 0 & \sigma_{\varepsilon_3}^2 & 0 & 0 \\ 0 & 0 & 0 & \sigma_{\varepsilon_4}^2 & 0 \\ 0 & 0 & 0 & 0 & \sigma_{\varepsilon_5}^2 \end{pmatrix}$	16 / 20

Table S3. Results of variance-covariance models for synchrony analysis. The table lists Akaike and Bayesian information criteria (AIC / BIC). The selected variance-covariance (VCOV) structures for modelling synchrony patterns for the study period (1901–2003) and for each 50-yr moving interval are in bold.

Period	*Broad evaluation*	*Narrow evaluation*	*Compound symmetry*	*Heterogeneous Toeplitz*	*Heterog. Toeplitz with two bands*	*Heterog. Toeplitz with three bands*	*Unstructured*
Study period							
1901–2003	–1714.9 / –1709.6	–1773.9 / –1747.4	–1776.8 / –1758.3	–1781.2 / –1744.2	**–1785.9 / –1756.8**	–1785.0 / –1753.3	–1782.4 / –1729.5
Moving intervals							
1901–1949	–775.7 / –771.9	–814.7 / –797.5	–803.5 / –790.1	–817.1 / –794.1	**–816.7 / –795.6**	–817.8 / –796.8	–817.0 / –780.7
1905–1954	–804.9 / –801.0	–836.4 / –819.2	–827.2 / –813.8	–802.7 / –775.9	**–837.3 / –816.3**	–835.5 / –812.6	–833.6 / –797.3
1910–1959	–765.9 / –762.1	–797.5 / –778.4	–793.6 / –780.2	–804.4 / –777.6	**–806.1 / –785.1**	–805.2 / –782.3	–808.7 / –770.4
1915–1964	–776.0 / –772.2	–796.3 / –779.1	–793.4 / –780.0	–802.7 / –775.9	**–806.6 / –785.6**	–805.3 / –782.4	–813.4 / –777.1
1920–1969	–776.7 / –772.9	–796.2 / –777.1	–796.3 / –783.0	–805.7 / –778.9	**–809.1 / –788.1**	–808.1 / –785.1	–813.6 / –775.3
1925–1974	–798.6 / –794.8	–828.7 / –809.6	–828.2 / –814.8	–836.5 / –809.7	**–839.1 / –818.0**	–838.0 / –815.1	–839.2 / –801.0
1930–1979	–815.2 / –811.3	–851.0 / –831.9	–854.1 / –840.7	–853.9 / –827.2	**–858.0 / –836.9**	–856.0 / –833.0	–849.9 / –811.6
1935–1984	–827.5 / –823.7	–859.9 / –840.8	–864.8 / –851.4	–865.6 / –838.8	**–869.6 / –848.6**	–868.9 / –845.9	–863.1 / –824.9
1940–1989	–794.6 / –790.8	–830.8 / –811.7	**–835.8 / –822.4**	–834.4 / –807.7	–837.2 / –816.2	–838.1 / –815.2	–829.0 / –790.8
1945–1994	–790.3 / –786.5	–819.8 / –800.7	**–827.8 / –814.5**	–820.0 / –793.2	–823.8 / –802.8	–823.7 / –800.7	–812.1 / –773.8
1950–1999	–784.0 / –780.2	–815.5 / –796.4	**–827.0 / –813.6**	–821.3 / –794.5	–823.0 / –802.0	–825.0 / –802.1	–814.0 / –775.8
1955–2003	–738.7 / –734.9	–760.1 / –741.2	**–774.0 / –760.7**	–765.4 / –738.9	–767.2 / –746.4	–768.4 / –745.7	–757.4 / –719.6

Supplementary Figures

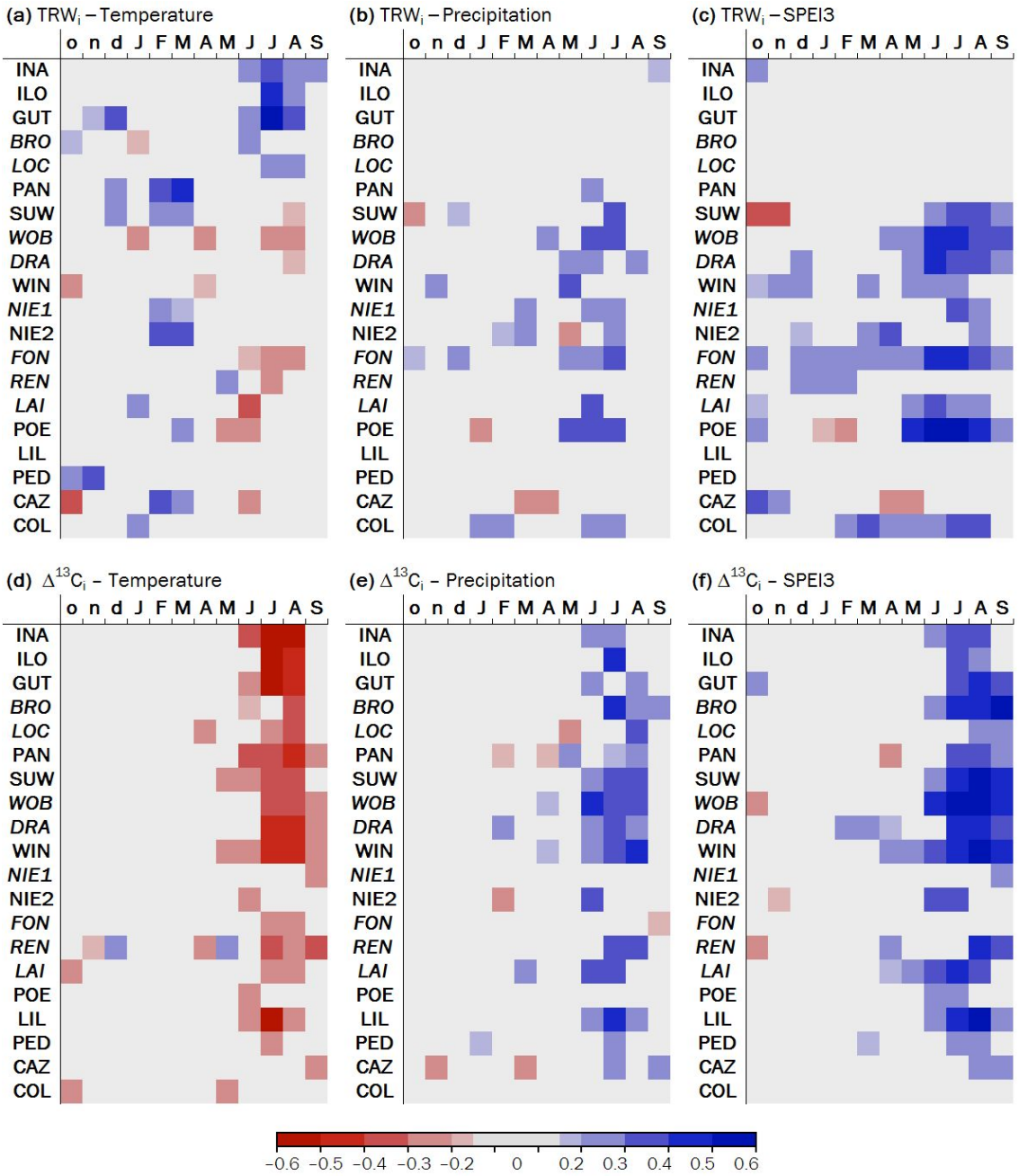

Figure S1. Climate signals at the site level for **(a, b, c)** TRW_i, **(d, e, f)** $\Delta^{13}C_i$ for the period 1901–2003. Tree responses to climate are based on bootstrapped correlations between tree-ring chronologies and monthly mean temperature (*left panel*), precipitation (*middle panel*) and 3-month Standardized Precipitation Evapotranspiration Index (SPEI3; *right panel*). Red and blue colors denote negative and positive relationships, respectively. Only significant correlations ($P < 0.05$) are shown. Sites are sorted latitudinally, from north (top) to south (bottom). Lowercase and uppercase letters correspond to months of the years before and during tree-ring formation, respectively.

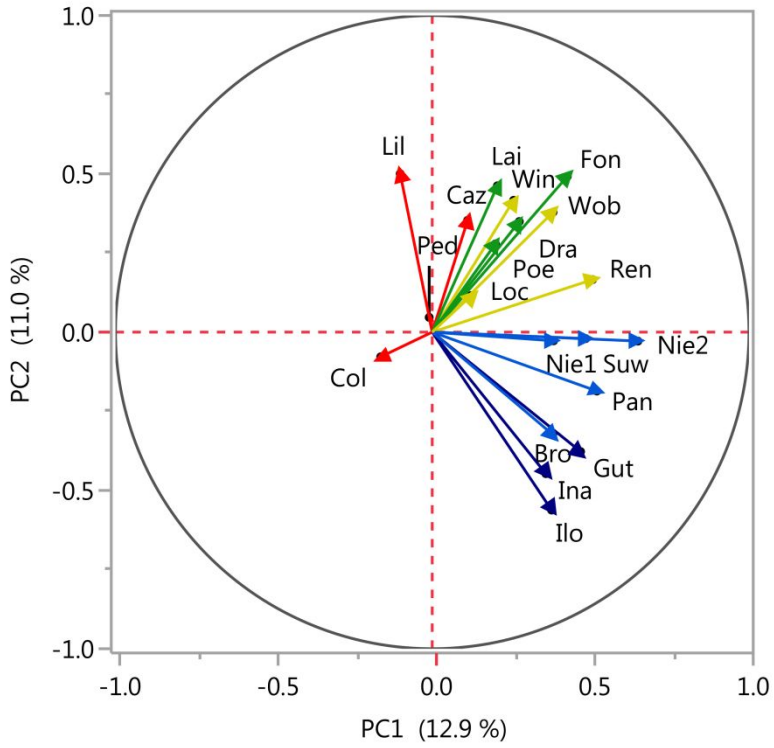

Figure S2. Principal component analysis performed on 20 indexed ring-width chronologies distributed across Europe and northern Africa for the common period 1901–1998. The biplot shows the loadings of the first and second principal components (PC1 and PC2) for each chronology. Colors indicate different groups as in Fig. 2. Codes are as in Table S1.

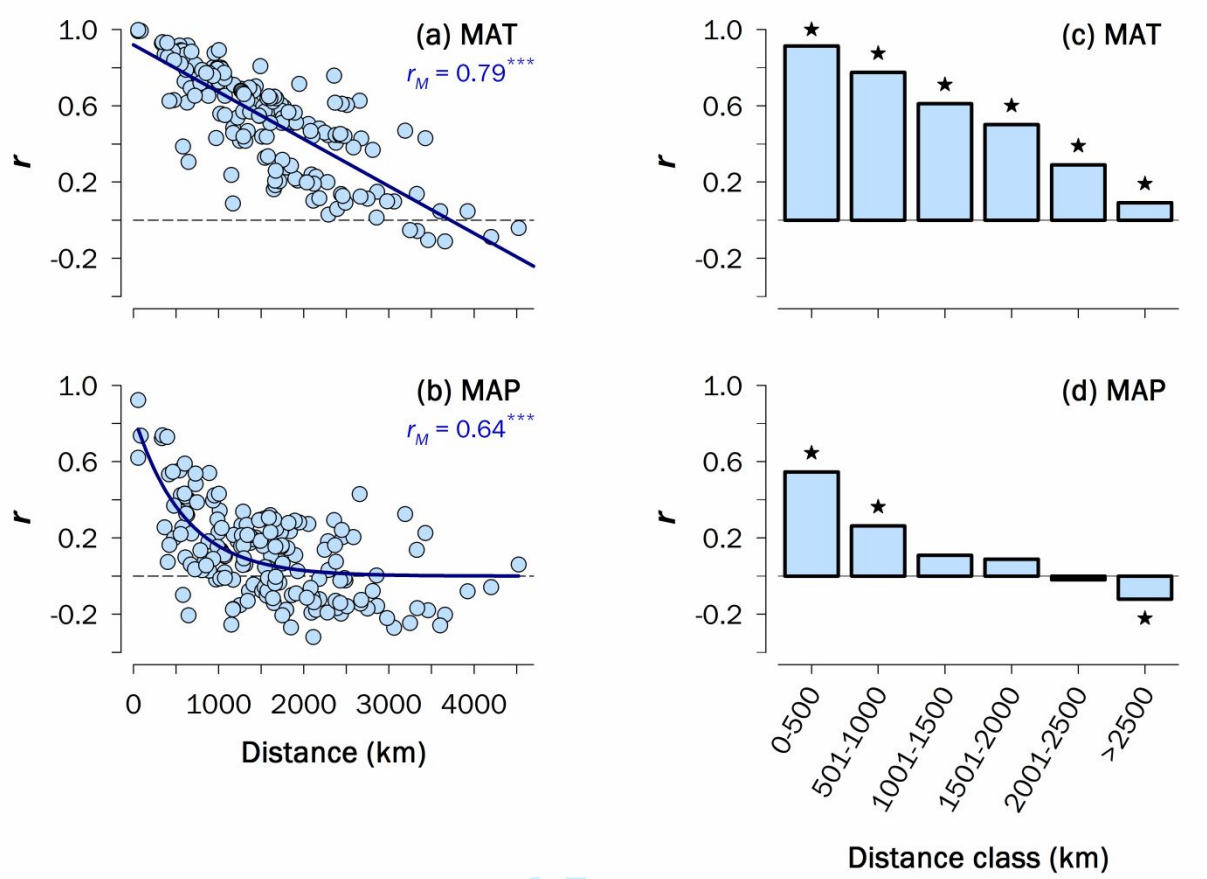

Figure S3.Spatial patterns of climate signals across Europe for the period 1901–2003: **(a, c)** mean annual temperature, MAT, **(b, d)** mean annual precipitation, MAP. Site climate series were obtained from the nearest grid point to each sampling site based on CRU TS 3.21 data. The resulting series were then subjected to linear detrending and autoregressive modelling to remove long-term trends (e.g., global warming) and serial autocorrelation, respectively. *(Left panels)* Pairwise correlations of climate series as a function of geographical distance. The patterns are summarized by regressing the correlation coefficients (*r* values) involving pairs of temporal series (*y*-axis) on their corresponding distance (*x*-axis) by using a linear function for MAT and a negative exponential function ($y = be^{-cx}$) for MAP. Asterisks after the correlation coefficient (rM) indicate level of significance based on a Mantel test ($^{***}P < 0.001$). *(Right panels)* Spatial structure of climate patterns across Europe. The spatial autocorrelation in the climate network was characterized for six consecutive distance classes (listed on the *x*-axis). Mean *r* values and their statistical significance (*P*) within each distance class were estimated from 1,000 randomizations. Significant correlation coefficients ($P < 0.05$) are indicated by asterisks.

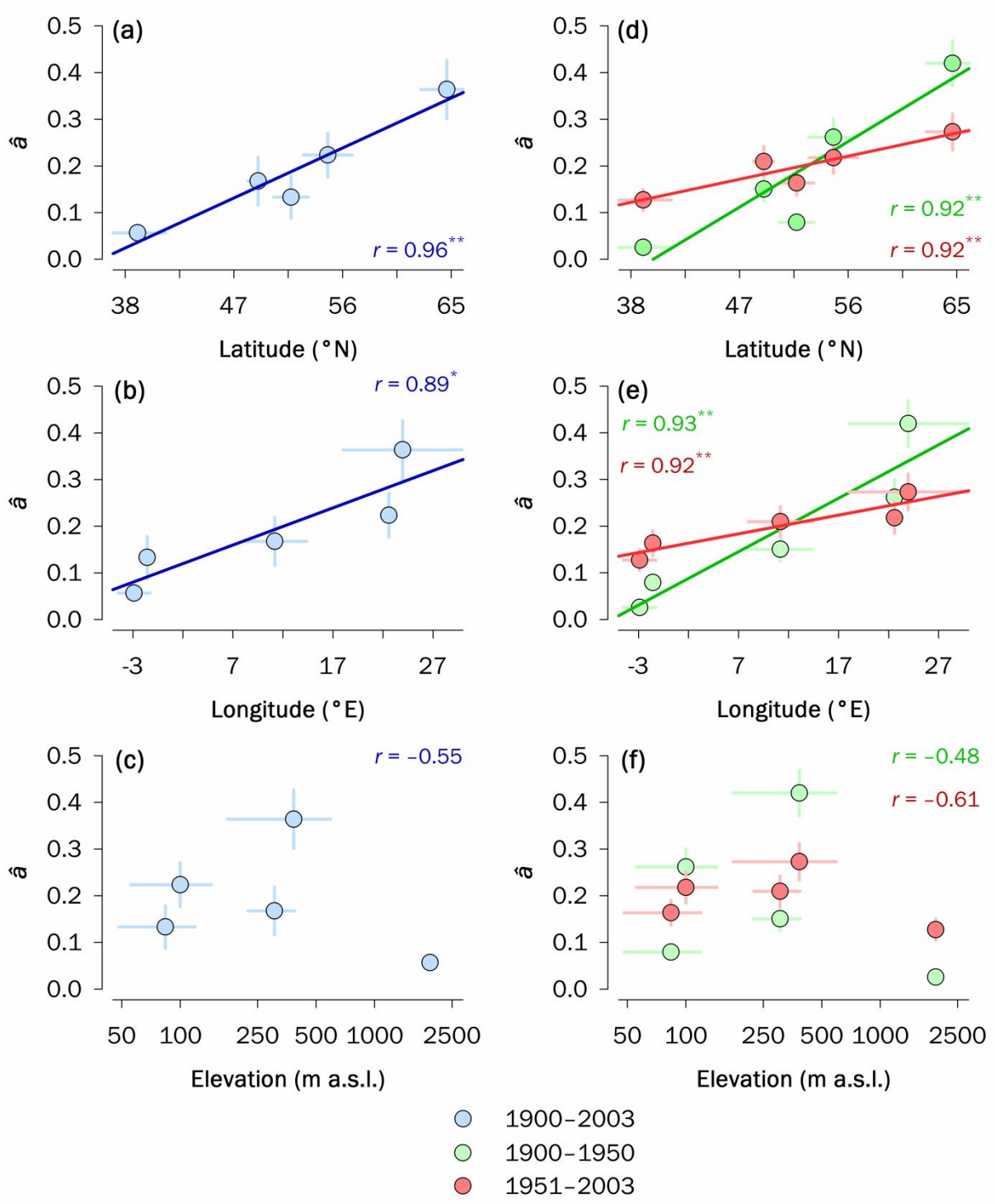

Figure S4. Geographical patterns of growth synchrony (*â*) at the group level for the entire period 1901–2003 and change in *â* for two consecutive periods (1901–1950 and 1951–2003).

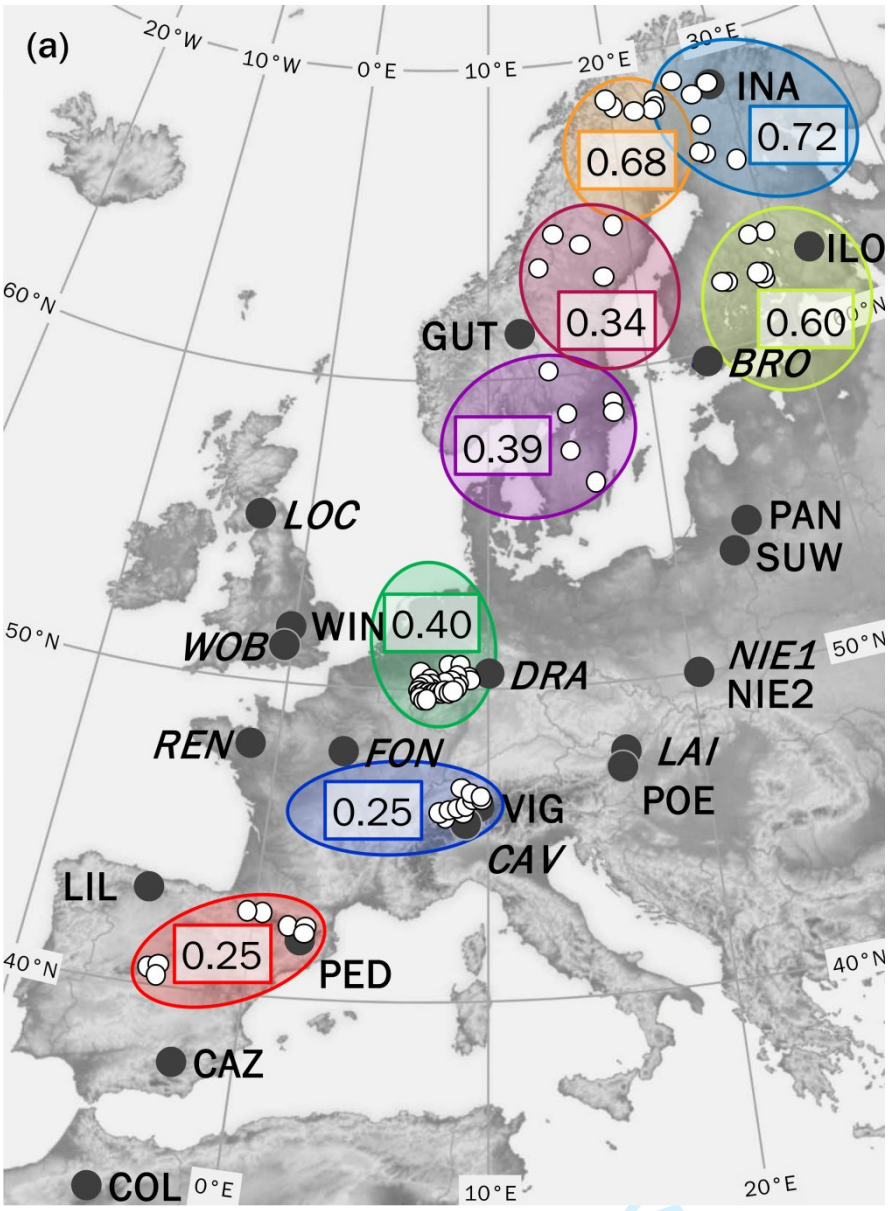

Figure S5. Geographical distribution of indexed tree-ring width chronologies for two independent datasets: pan-European network ISONET (black dots) and the International Tree-Ring Data Bank (ITRDB; Grissino-Mayer & Fritts [1997]) (white dots) for the period 1901–2003. Colored circles identify eight groups of neighbouring chronologies (n= 80) obtained from ITRDB. Numbers indicate growth synchrony ($\hat{a}$) at the group level. The criteria for inclusion in the analysis were: (*i*) geographic coverage = European continent; (*ii*) time span = 1901–1998 or larger (common time period for ISONET chronologies); and (*iii*) taxonomy = same species of ISONET network. The chronologies that could be classified into groups given the requisite of 1,000 km as maximum distance between site chronologies were finally selected. Indexed ring-width chronologies were built for each site following the procedure described in Materials and Methods of main text.

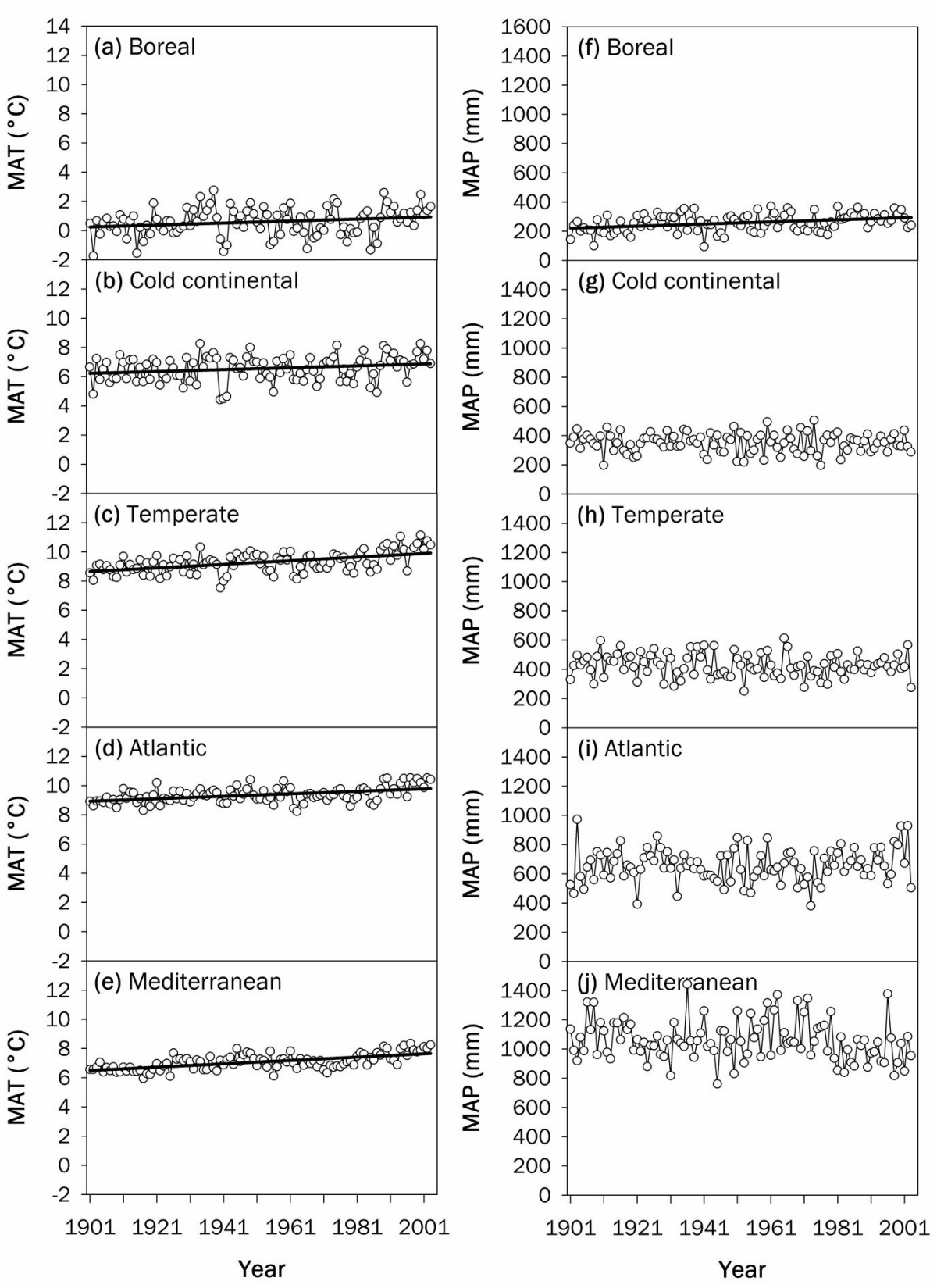

Figure S6. Trends in climate parameters at the group level: **(a-e)** mean annual temperature (MAT) and **(f-j)** mean annual precipitation (MAP). Significant linear trends along the climatic gradients are depicted as thick lines ($^{*}P < 0.05$).

Response letter to the reviewers and associated editor

(Global Ecology and Biogeography GEB-2018-0520)

Spatiotemporal patterns of tree growth as related to carbon isotope fractionation in European forests under changing climate, by Shestakova *et al*.

First of all, we would like to sincerely acknowledge the editor and two anonymous reviewers for their comments, suggestions and corrections, which have been extremely useful to improve the manuscript. The text has undergone extensive revision guided by their ideas, focusing further on the interpretation of our results and simplifying the storyline to make the article more attractive to readers of GEB. We hope this version meets the high standards of the journal, as we are satisfied to have produced, in our opinion, a largely improved version over the previous draft.

Note: the line numbers included in the responses below refer to the blind-review version of the manuscript.

EDITOR'S COMMENTS TO AUTHOR

Editor: Hickler, Thomas

The authors analysed trends in tree growth inferred from a European network of tree ring data. The trends were analysed in terms of their correlation with climate trends and coupling with leaf gas exchange (delta 13C), which to my knowledge has not been done at this scale across Europe and allows interpretation in terms of water stress. The topic is highly relevant and fits to GEB, and the manuscript is generally well written and presented (but see very critical comments by reviewer 2). The results in terms of spatial patterns broadly confirm what one might expect, but the quantification and some details are, nevertheless quite interesting.

A: We thank the editor for this positive reception of our work. Indeed, as far as we know, an extended analysis of the nature and magnitude of ring-width *vs.* $\Delta^{13}C$ coupling across Europe has not been performed thus far. In order to face in a convenient way most reviewers' suggestions, which clearly ask for extra space in the manuscript, we have included the information of previous Figures 3 and 5 in the new Figure 1. The saved space has been used to increase the extension of the text and references. In its current form, the manuscript has 4 figures (instead of 6 figures) and 1 table, 6140 words and 66 references. We hope these numbers are suitable for GEB.

The logical flow from hypotheses to conclusions, however, could be improved. I would suggest to formulate the hypotheses more mechanistically and then to derive which patterns would be expected to confirm or reject the hypotheses (instead of using the predictions as hypotheses). Note that I found many comments from the very critical reviewer 2 convincing, and I also agree on the comments by reviewer 1. To fully address all reviewer comments, a major revision is necessary, probably also including additional analyses or, at least, modifications to the presentation.

A: Thanks for the suggestion. We have reformulated the hypotheses using a more mechanistic approach:

"We hypothesise that, on a continental scale, (i) temperature exerts – as a consequence of its large spatial homogeneity – a greater influence than drought on the spatial signals imprinted in tree rings; (ii) the relationship between ring-width and $\Delta^{13}C$ reflects the relative significance of carbon assimilation and stomatal regulation on tree performance, with positive relationships reflecting photosynthesis limited by stomatal conductance at low- and mid-latitude sites, and negative relationships suggesting temperature- or light-limited carbon uptake at high-latitude sites; and (iii) widespread warming-induced drought stress triggers a tighter stomatal control of water loss that strengthens the relationship between growth and $\Delta^{13}C$ at low- and mid-latitude sites, as the stomatal sensitivity to drought becomes more limiting for carbon uptake. Therefore, we predict more synchronous growth linked to coordinated stomatal responses across species and regions as the climate becomes warmer and drier along the latitudinal gradient."

In addition to the reviewer comments, which should be addressed before considering the manuscript for publication in GEB, I have the following suggestions to improve the manuscript.

Q: *Abstract: end of Methods: statistical method could be deleted.*

A: The reference to the statistical approach used has been deleted of the Abstract.

Q: *End of Results in Abstract (and associated text in Conclusions): Does the increased coupling really apply across Europe? I don't see this clear trend in figure 6 and it contradicts the higher importance of temperature trends in the north. This point is important because it is highlighted as a major result, indicating more drought stress across Europe.*

A: We agree with this comment. The increasing coupling (i.e., relation turning into significantly positive at the turn of this century) applies to three out of the five climate types (Mediterranean, temperate and cold-continental), whereas the Atlantic group remains unaffected and the Boreal group shows decoupling (i.e., relation changing from negative to non-significant) (see Fig. 4). This sentence was misleading and it has been corrected. In fact, the Results and Conclusion subsections of the Abstract have been very much revised to the light of the comments of the reviewers, and we hope they now reflect better the scope of our study.

Q: *At least partly similar analyses have been carried out by Babst et al. and Shestakova et al. When these are mentioned in the introduction, the similarities to these studies (e.g. data used by Babst et al.) and the advances presented here should be described in more detail. As the findings from these two studies are relevant to describe the state of the art, also the main findings should be described shortly already in the introduction.*

Also in the discussion, the results here could be compared in a bit more detail to those of Babst et al.

A: We also agree with this comment. As suggested, the main findings of these studies have been described in the Introduction (L. 71-75 of the new version) to better frame our work. Also, our results are now compared against those of Babst et al. (2013) in the Discussion (L. 449-456).

Q: *Minor: Introduction (Nabuurs et al. 2013), did surely not refer to "natural forests", which hardly exist in Europe.*

A: The comment is pertinent; we basically wanted to refer here to "old" logged forests which have remained untouched at least for the last 50 years. In any case, the wording has been modified as to avoid any confusion (L. 57).

Q: *Finally, reviewer 2 suggests making the data available, which I surely encourage, but I have not yet checked the GEB policy on this.*

A: Raw TRW records will be available at the International Tree Ring Data Bank (ITRDB) provided the paper is published. $\delta^{13}C$ records are available as Supporting Information in Treydte et al. (2007), grl23621-sup-0003-fs02.eps file (freely accessible at https://agupubs.onlinelibrary.wiley.com/doi/full/10.1029/2007GL031106).

We have included this information in the Data Accessibility Statement of the manuscript.

Reviewers' comments:

Reviewer #1.

General comment: *The authors analyzed the spatio-temporal variability in the synchrony of radial growth rates and Δ13C across Europe. The database and statistical methods used for that purpose are appropriate, the paper is well written, and should be of the interest of a broad community.*

A: Many thanks to the reviewer for this encouraging comment on our manuscript.

Q: *In addition to some minor comments, 2 aspects should be considered before the paper can be accepted.*

Methods: I'm not sure that including the site COL from Morocco is appropriate. First, this is the only site with cedar, which is definitely not a Pinus (see L105) and does not have the same strategy than this genus. Second, based on the PCA (Fig. S2); it is clear that the growth time- series in COL strongly differs from the other ones, including the Mediterranean ones. Thus, including this site automatically decreases the growth synchrony within the Mediterranean group, which may bias the overall interpretation of the results [even though similar results are obtained with the ITRDB database, I would exclude COL]. Note also that each site from the Mediterranean group focuses on

a different species (P. nigra, P. sylvestris, P. uncinata, Cedrus atlantica), which may contribute to the low synchrony…

A: We understand the concern of the reviewer. In fact, we were also troubled about whether to make use of the only *Cedrus atlantica* chronology (COL) at the southernmost site of the network. However, we think there are strong reasons to keep the cedar chronology in the analysis. First is that this site is one among the original 23 sites of the European network ISONET. Accordingly, all previous published works using the ISONET dataset have included COL, namely: the analysis of the temporal coherence and common climate signals in the isotopic network (Treydte et al. 2007), the characterization of the spatial variability and temporal trends in water-use efficiency (Saurer et al. 2014), and the quantification of changes in transpiration over the 20th century (Frank et al. 2015). Second, unlike the three discarded sites of the network, COL is classified into the same climate type of its neighbour chronologies (PED, LIL, CAZ) within a geographical distance of 1,000 km (limit for temporally coherent ring-width signals in the network; Figure 2). Third, *Cedrus atlantica* is likely a conifer of Euro-siberian origin (like the pines in the network), as suggested based on genetic evidence (Qiao et al. 2007), which indicates that the Mediterranean group is less heterogeneous than it can be initially expected (L. 147). Fourth, *Cedrus atlantica* is a *Cedrus* species with stomatal behaviour close to the Eurosiberian pines of the network; at least the closest among *Cedrus* spp. (L. 448-449): species-specific differences in water potential (Ψ) thresholds for stomatal closure are as follows: -2.4 MPa in *C. atlantica* (Ladjal et al. 2007), -2.0 to -1.6 MPa in *Pinus nigra* (Froux et al. 2002), and -1.4 to -1.0 MPa in *P. sylvestris* (Irvine et al. 1998). In comparison, stomatal conductance still remains at significant and constant levels below -2.4 MPa in the two oaks present in the network, *Quercus robur* and *Q. petraea* (Bréda et al. 1993), in agreement with their anisohydric performance. Fifth, and finally, it is true that COL departs the most from the remaining chronologies in the PCA (Fig. S2), but this could be just a consequence of its geographical position very far apart from the majority of the sites. If a new PCA is build using only the four Mediterranean sites, COL does not stand out for its distant placement in the biplot (Fig. R1). In fact, all four sites are about the same distant, meaning that their performance is relatively different (i.e. they show low growth synchrony). This result is supported by the independent analysis of records from the International Tree Ring Data Bank (Fig. S4),as well as by other published evidence demonstrating low synchrony among mountain forests in the Iberian Peninsula (Shestakova et al. 2016).

In summary, all these evidences make us be confident enough as to keep COL in the analysis. As mentioned, the third and four lines of evidence have been included in the text.

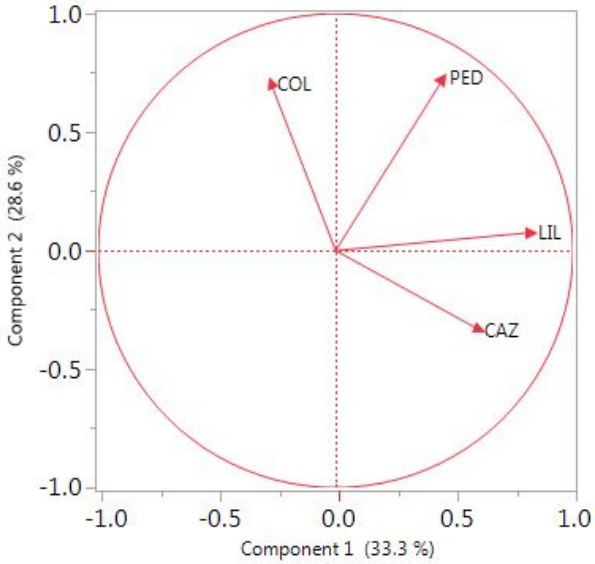

Figure R1. Principal component analysis performed on four indexed ring-width chronologies distributed in the Iberian Peninsula (PED, LIL, CAZ) and Morocco (COL) for the common period 1901-1998. Codes are as in Table S1 on the submitted manuscript.

Q: *Discussion: Something that really misses in the interpretation of the results is related to the source activity (photosynthesis) – sink activity (cambial activity) control of tree growth. Even though briefly mentioned in L462-467, the authors tend to forget that environmental stress constrains sink activity before it affects source activity (see Körner 2014 Curr. Opinion Pl. Biol.), and this explains part of the de-coupling between leaf- and stem-level processes (L361). Environmental stress also changes C allocation patterns, but this may be a less important aspect. Please better consider this point, especially in the sections L111-113; L360- 365; L398-414; L427-432.*

A: This comment is very important and we would like to acknowledge the suggestion of the reviewer. Indeed, we agree that the issue of sink activity *vs*. source activity had been overlooked in the previous version. We have commented on the roles and feedback between sink and source to better frame and interpret the increasing coupling between TRW and carbon isotopes over time observed in most continental Europe. In this way, we have softened our initial statement that stomatal regulation of photosynthesis is progressively *controlling* tree growth owing to increased drought effects (as main justification underlying the observed coupling). For example, see L. 95-98 (Introduction), or L. 428-431, L. 487-490, L. 524-526, L. 532-534, L. 558-559 (Discussion). In this way, we believe the paper has gained in focus and strength.

Other comments:

Q: *L59: "climate change and increased atmospheric CO2 (atmCO2) have largely altered the growth of natural forests (…) research efforts have been mainly confined to local ecosystems ». This is not entirely true, there are some studies carried out at continental scale: e.g., Girardin et al. 2016 PNAS; Pretzsch et al. 2014 Nat. Comm.*

A: We agree that this sentence is not exact, although we tried to avoid oversimplification (i.e. 'mainly confined'). The sentence has been re-elaborated as follows: "To explore these dynamics, research efforts have been usually confined to local ecosystems, with some representative woody species and their interactions examined at small spatial scales (but see e.g. Pretzsch et al., 2014; Girardin et al., 2016)."

Q: *L86: "in temperate forests thriving under near-optimal conditions, where tree growth patterns may not be informative of climate variability". I do not agree: climate events strongly impact the productivity and structure of temperate forests. Please look at Pederson et al. 2014 Ecol. Monog., or Martin-Benito et al. 2018 Glob. Ecol. Biogeo.*

A: The reviewer is right. We have changed the sentence as follows: "This is especially relevant in temperate forests thriving under near-optimal conditions, where tree growth fluctuations may not be as sensitive to climate factors as stable isotopes (Hartl-Meier et al., 2015)."

Q: *L87: "environmental variables". This is too vague, please detail*

A: We wanted to refer basically to climate variables, as stated e.g. in Hartl-Meier et al. (2015). Therefore, we have replaced 'environmental variables' by 'climate factors'. Please see the previous query.

Q: *L92-100: here and/or in the discussion, I would discuss the limit of using Δ13C alone as indicator of the stomatal regulation strategy. Combining Δ13C and Δ18O information provides better insights on the relationship between stomatal conductance and C assimilation (see Scheidegger et al. 2000 Oecologia; or Gessler et al. 2018 New Phytol.)*

A: We agree with this comment. A combined analysis of $\Delta^{13}C$ and $\delta^{18}O$ records in the same network can be found in Treydte et al. (2007). Interestingly, these authors report strong similarities in the response of carbon and oxygen isotope records to summer moisture conditions across the network, suggesting a tight link at the leaf level mediated through variation in stomatal conductance caused by the combined effect of varying temperature and precipitation conditions (i.e. in line with Scheidegger et al. [2000]). This relevant information, which indeed reinforces our interpretation and conclusions, has been included in the Introduction (L. 106-110).

Q: *L95-97: RW is also affected by changes in irradiance, phenology etc… please modify*

A: We agree with reviewer. To qualify this idea, we have slightly modified the corresponding sentences by including 'primary' and 'progressively' (underlined below). The recognition of additional factors driving variability in RW is mentioned immediately after in the text:

"Under such conditions, radial growth and $\Delta^{13}C$ are bound together by two primary factors: stomatal regulation and water availability (…). However, $\Delta^{13}C$ is progressively

affected by changes in photosynthetic activity associated with irradiance, phenology or nutritional stresses when water becomes less limiting."

Q: *L109-111: please mention here or elsewhere that the lack of synchronous growth in drought- prone forests depends on the spatial scale of the analysis. At continental scale, I fully agree and the results of the present study support this pattern. However, at local scale, this may not be the case -> high RBAR; see Fritts 2012)*

A: This is an important point and we agree with the reviewer comment. We have qualified further the interpretation of patterns of synchronous growth in the Discussion section (L. 443-445): "...hence resulting in substantially less synchronous growth occurring at large spatial scales (Shestakova et al., 2016)."

Q: *L220: why is the SPEI3 used? Was there any preliminary analysis that justifies the use of SPEI3?*

A: Yes. We chose SPEI3 instead of SPEI1 because SPEI1 shows about the same information as monthly precipitation, while SPEI3 integrates the water deficit occurring on a longer (seasonal) term. In particular, the three-month SPEI was selected because June-August was the period of highest climate responsiveness across the network for both TRW_i and, especially, $\Delta^{13}C_i$ (Fig. S1). This explanation has been included in the text (L. 221-223).

Q: *L234: which PET equation was used?*

A: We used the Hargreaves equation (Hargreaves and Samani, 1982). This reference has been added to the text (L. 215-216).

Q: **L239: usually PET is highly correlated with T, so I'm wondering why you found a positive correlation between PET and elevation, while this was not the case between T and elevation…**

A: In fact, the correlation between T and elevation was marginally significant ($P < 0.10$), and as such was not explicitly mentioned in the text. Of course, it can be included if deemed necessary.

Q: *L246: I'm not so fan of analyzing trends in BAI to compare growth trends among sites with different sampling characteristics (e.g., different age and size distribution). Age/size effects also remain in BAI data. Could you also detrend the BAI data using a RCS standardization method (that preserves low frequency variation) and calculate the trends on the residual chronologies?*

A: This is indeed an issue of debate in the dendrochronology community. There is not an optimum solution to face the problem of optimum standardization to preserve low frequency variability. Since we calculate BAI trends using old-growth trees (age well above 200 years already at the beginning of the 20th century in most cases; Table S1),

we assume that these trends are free of age / size effects. Indeed, this approach minimizes the transitory dynamics associated with stand development and succession. As suggested elsewhere, standardisation is not always really needed: in tree-ring series of trees selected in the classical dendrochronological way (i.e. the tallest and oldest trees in a stand), the most recent part of the growth curve (corresponding to years when trees have already reached their maximum height) usually shows no ontogenic trends (Carrer et al. 2016, 2017). However, we have checked the validity of our results through RCS as suggested by the reviewer, and the resulting analysis has been included in the text replacing the former one (L. 196-199 [M&M] and L. 309-312, L. 509-512 [Results]). The results are similar to those of former version, with growth enhancement observed in a restricted number of chronologies (5) from high and mid latitudes, and no growth stimulation for the remaining 15 chronologies.

Q: *L299-301: should be part of the M&M?*

A: This sentence has been dropped from the text as part of our efforts to streamline the manuscript.

Q: *L326: the analysis of the synchrony in climate variables is an important aspect of the entire analysis, so I would show the in Supp. Mat.*

A: The analysis of synchrony in climate variables is shown in Figure R2, where no obvious trends over time can be observed. We have opted to not to include this information in Supp. Mat. for the sake of easier readability of the study following the suggestion of reviewer #2. In fact, the Supplementary Information has been very much simplified, with some relevant material now included in the main text. On the other hand, some Figures and most sections of Supp. Mat. that are not strictly needed to follow the work have been eliminated. Of course, we are open to add this figure if the reviewer prompts us to do so.

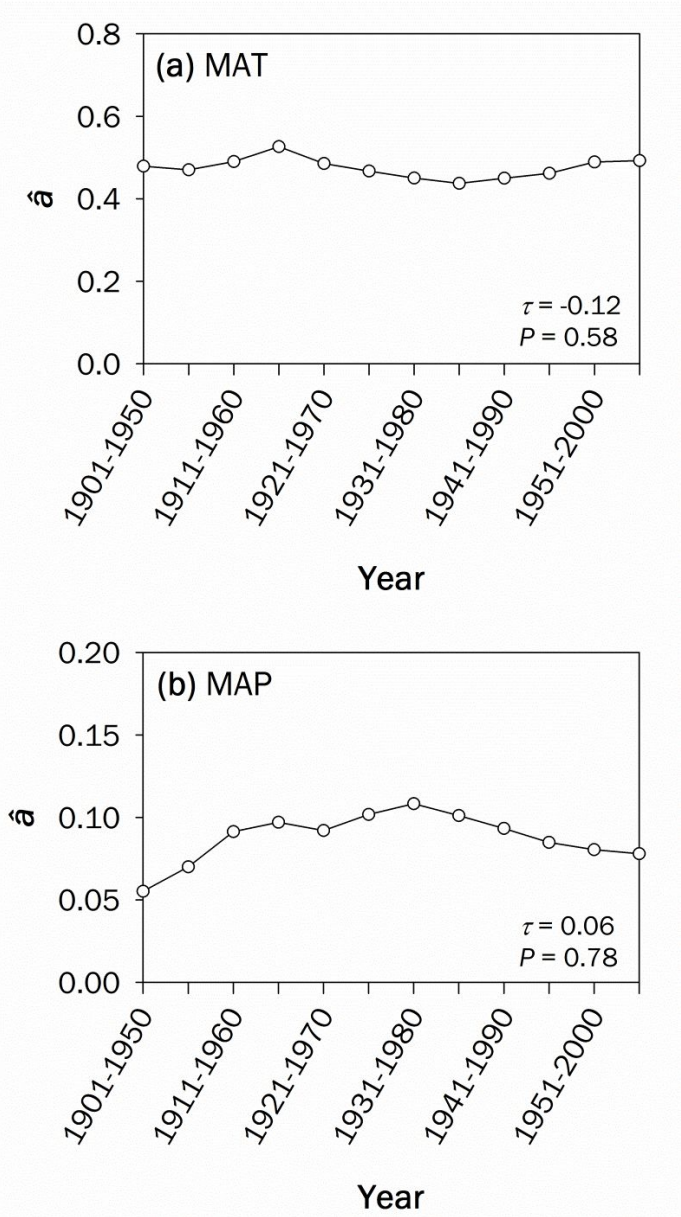

Figure R2. Evolution of synchrony in (a) mean annual temperature (MAT) and (b) mean annual precipitation (MAP) using climate data from the nearest grid point of each site of the high-resolution climate dataset (Climatic Research Unit, CRU TS 3.21). The significance of synchrony trends is assessed using the Kendall (τ) non-parametric test.

Q: *L398: "The positive relationships between TRWi and Δ13Ci at low and mid latitudes suggest that stomatal limitation of leaf carbon assimilation is a key mechanism controlling tree growth synchrony". Not entirely, this also suggest that the same environmental driver (e.g., drought) controls the inter-annual variability in both variables.*

A: We agree. The beginning of this paragraph (L. 479-482) has been modified as follows: "For the entire study period, the positive relationship between TRW_i and $\Delta^{13}C_i$ in low and mid latitudes indicates that leaf-level physiology and tree growth are commonly driven by water stress, to a greater or lesser extent, south of ≈60°N in

Europe (Fig. 1). Therefore, it suggests that stomatal limitation of carbon assimilation is imprinted in tree growth at most of the study area …"

Q: *Table 1: what does the column "MAP<PET" indicates?*

A: It refers to the period when PET exceeds mean annual precipitation at the site level. This was unclear and has been modified in the table.

Q: *Figure 3b: I do not understand why the synchrony equals 0 for some group pair… Is it equal to zero, or close to zero?*

A: This result stems from the identification and further application of the best variance-covariance (VCOV) model underlying the TRW_i records, which is thereafter used to retrieve synchrony estimates at the within- and between-group levels. This is indicated in the Results section: "A heterogeneous Toeplitz with two bands was the best VCOV model for the period 1901–2003, indicating covariation between neighbouring groups only (Table S3)" (L. 352-354). For this reason, non-neighbouring groups have synchrony that can be effectively taken as zero. In the current version of the manuscript the results displayed in Figure 3 (and also those of Figure 5) have been incorporated into Figure 1. This issue has been addressed in the figure caption to make it clear.

Q: *Figure 4: there is an issue with the x-axis, which is probably not correct: 1901-1972 instead of 1901-2003 (or part of the data is missing?)*

A: The reviewer is right. We apologize for this mistake. The figure has been corrected accordingly (now Figure 3).

Q: *Figure 5: for p<0.1 values, I would use a dot rather than an asterisk. Also, the error bars are not so visible...*

A: The information presented in this figure has been incorporated into the current Figure 1. Correlation estimates between TRW_i and $\Delta^{13}C_i$ at the group level (r_Y) are shown in the figure (insets) together with their SE, and the scatterplots show year-level estimates (BLUPs) of TRW_i and $\Delta^{13}C_i$ extracted from the bivariate mixed models. The significance of these correlations is indicated by a straight line in the scatters: "Significant correlations (those having confidence intervals which not straddle zero, 90% CI approximated as $r_Y \pm 1.64SE$) are indicated with lines." Please note that the high SEs of the correlations (r_Y) stem from the error behind BLUP predictions that is carried forward in a bivariate model using REML (Houslay & Wilson, 2017) (L. 805-807). The redrawn Figure 1 originates from a request of reviewer 2 asking for "a spatial analysis or map of the strength/nature of the $\Delta^{13}C_i$:TRW_i relationship".

Q: *SuppMat, P31-L20: I'm wondering to which extent using the whole ring to quantify Δ13C for conifers, and only latewood for oaks can lead to non-synchronous results between oaks and conifers? Can you discuss that aspect?*

A: The comment is pertinent and, in fact, this possibility was examined in detail by Treydte et al. (2007). They reported that previous year climate conditions did not have a strong effect on carbon isotope values, and they discussed that this finding was somewhat expected for the latewood cellulose from oaks, but also held for pines (whole ring cellulose). Thus, the results do not indicate substantial carry-over effects in conifers due to remobilized reserves from previous summer. Treydte et al. (2007) concluded that the extent and nature of the climate signals recorded in the isotopic network did not show obvious species-specific differences (Abstract in Treydte et al. [2007]). This relevant information has been included in the paper (Material and Methods section, L. 183-185).

Q: *SuppMat, P31-L53 to P32-L5: I would move this section to the main text*

A: Done.

Q: *SuppMat, P31-L17-24: please do not use mean RW (mm/year) to quantify mean growth rate: this metric highly depends on tree size (see Bowman et al. 2013 Trends Pl. Sci.).*

A: This sentence has been dropped from the manuscript in order to streamline the message (following the suggestions of reviewer #2). Indeed, this is not crucial information contributing to the significance of the study.

Reviewer #2.

Q: *The work that went into the collection and analysis of these data appears to be of high quality. Unfortunately the manuscript suffers from several problems which make it very difficult to assess whether the conclusions drawn are robust. There are however potentially important findings in this analysis.*

A: We thank the reviewer for highlighting the flaws and weak points of our manuscript. Based on her/his ideas we have tried to improve the storyline of the study; we hope that this new version delivers conclusions that are robust and valuable.

Q: *One major scientific uncertainty is the nature of the relationship between TRWi and D13c. This relationship is set up as an important and novel contribution of the paper. While the statistics of this relationship are reported in summary form, no plot showing these two variables is provided. I found no analysis testing whether a linear fit rather was the most parsimonious fit for these variables. Depending on how TRWi was calculated some sort of curvilinear fit might be expected. The hypotheses reply on understanding this relationship, the relative strength of this relationship between species, across regions and climatic zones. It should be fully explored.*

A: We regret the important issue of standardization was unclear in the manuscript. This information is now included in the main text (taken from Supplementary Information). Both traits (TRW, $\Delta^{13}C$) were standardized to preserve high-frequency

variability (L. 166-171, L. 187-188) and therefore they are stationary (mean=1, common variance). This means that a curvilinear fit for the relationship between TRW_i and $\Delta^{13}C_i$ cannot in principle be expected. Figure 1 shows the relationships between both traits at the group level.

Q: *A second scientific concern is whether the sampling is sufficiently even to rely of tests between geographic areas with different species. A single pine species at a single site made up nearly 36% of the trees sampled, though this detail was difficult to work out from the methods. These different species (or at least the two genera) are likely to have very different stomatal responses to drought (Hacke et al 2000, Klein 2014, Roman et al 2015) and the nature of the relationship between D13c and growth may well differ. The mixture of oaks vs pine individuals used in the analysis may influence how we should interpret the regional patterns.*

Seftigen, K., Frank, D. C., Björklund, J., Babst, F., & Poulter, B. (2018). The climatic drivers of NDVI and tree-ring based estimates of forest productivity are spatially coherent but temporally decoupled in Northern Hemispheric forests. Glob. Ecol. Biogeogr.

A: It is indeed true that the unbalancedness in sampling effort among sites was important. However, all site chronologies delivered EPS values over 0.85 for the 20th century, meaning that every chronology is representative of the site conditions according to well-known dendrochronological standards (L. xxx). Also, the issue of different functional types showing potentially different water use strategies is very relevant, and has been confronted in the text accordingly. An extensive reply to this particular issue can be found later in this rebuttal letter. Finally, the work by Seftigen et al. (2018) is relevant to justify, at least in part, the observed decoupling between leaf-level physiology and tree growth. As such, it has been incorporated to the Discussion section (L. 431-432).

Q: *The main concern in the manuscript in its current form is that the methods are vague to the point that I was unable to determine whether or not the conclusions were justified. Secondarily, the appendices are overly long and not tailored to this manuscript so that important information about the paper is obscured and confusing for the reader.*

A: We apologise for this vagueness. We were somehow constrained by the text extension allowed by GBE (up to about 5,000 words in main text), but it is indeed worrying that the methods were delivered so imprecisely. In order to solve this issue some extra space in the main text is needed. In this regard, we have decided to drop a couple of figures from the main document (former Fig. 3 and Fig. 5), namely the between-group synchrony values (former Fig. 3) and the relations between TRW_i and $\Delta^{13}C_i$ at the group level. The information has been incorporated into Figure 1 (e.g. insets in Fig. 1). Based on the saved space, and following the instructions of the journal which allows to trade figure / tables for extra text, we have included part of the meaningful information buried in Supp. Inf. (former Appendix 1 and 2) into the main

text (M&M section). Please, see details in the answers provided to the remaining queries of reviewer #2.

Q: *The methodology is not clearly explained in the manuscript. I believe it is relatively simple - an index of growth and an isotopic index were estimated for 20 trees of 5 different species across different geographic locations in Europe with contrasting climate and vegetation. Spatial and temporal statistics were carried out. Also these two metrics were correlated with each other and the strength of this correlation was assessed across different spatial scales and regions.*

A: The reviewer is essentially right. However, the sample size was much higher than barely 20 trees sampled across Europe. We used 20 site chronologies each of them composed of 7 to 326 trees (total = 891 trees; site mean = 46 trees; median = 28) (Table S1). Although the unbalancedness in sampling effort was important, all site chronologies delivered EPS values over 0.85 for the 20th century, meaning that every chronology is representative of the site conditions according to well-known dendrochronological standards.

Q: *I suggest starting the methods section with a broad and simple explanation of the steps with the sample sizes clearly defined to help the reader understand the overall methodology. This can be followed by detailed descriptions in sections as the authors have now.*

A: We acknowledge this suggestion. A simple explanation of the different methodological steps has been included at the beginning of the subsection of M&M labelled 'Analysis of spatiotemporal patterns of tree-ring traits: methodological steps' (L. 229-236). Afterwards, a detailed description on the different analytical steps follows in the same subsection. In this way, we hope the flow of the analysis is more clearly delineated.

Q: *I found it very difficult to follow some of the sections of the methodology, with critical details either vaguely defined, listed in appendices. For example TRWi is not defined specifically - it is introduced but the reader has to puzzle out for themselves what the term means and whether - the authors hint that it is BAI, but I am not certain. The spatial classes described around lines 153-157 are similarly vaguely explained.*

A: Again, we regret these important details went unnoticed in the former version. Information on how TRW_i (and $\Delta^{13}C_i$) was derived is now included in the main text (L. 161-194). TRW_i does not refer to BAI under any instance; instead, BAI is used to obtain long-term trends in absolute growth. This differentiation is crucial, and we hope it is made clear in the current version. The information on how BAI is calculated is now included in a stand-alone paragraph and, following reviewer #1, the BAI trends have been recalculated using a Regional Curve Standardization procedure to eliminate any potential bias stemming from differences in tree age across site chronologies. The results are similar to those of former version, with growth enhancement observed in a restricted number of chronologies (5) from high and mid latitudes, and no growth stimulation for most chronologies.

Q: *The authors describe the ISONET, which is a rich dataset but the description of what trees were used to derive the indices is difficult to find. From the main text, the reader does not know how many trees of each species were used in the correlations. You can derive numbers from Table 1 P sylv (8), Q rob (5) Q pet (3) P. nig (2), P unc (1), C atl (1).*

A: As previously stated, we have used 20 site chronologies, and each of them is composed of 7 to 326 trees. These trees belong to the site-species combinations included in Table 1. This information is included in the first subsection of M&M (L. 144-147).

Q: *The authors refer to 20 chronologies of old trees, which might suggest to some readers that only one or two old trees from each site was used. This confusion is compounded because the text describing how many trees of each species is vague (e.g. line 135 derived from numerous trees at each site Table S1). Only when the reader goes to appendix Table S1 can they discover that the sampling is highly variable between sites and species; while 15 sites represent between 1 and 5% of the trees sampled, 4 sites represent between 5-10% of the trees sampled and site 16 (Poe) comprises 36% of the sample (326 trees out of the 891 sampled).*

A: The term chronology refers to the standard dendrochonological concept of an average temporal tree-ring series made up of a number of representative trees (and grounded on the value of EPS over 0.85). We hope this notion is made clear in this new version. For instance, information on the mean number of trees per site is now included in the main text (L. 161-163). The unbalancedness in the number of trees per site is not a concern provided each site is sufficiently represented for the study period, as demonstrated by EPS site values exceeding 0.85 over the 20th century (L. 177-178).

Q: *The sites listed have only one species associated with them in Table S1 - however in Figure 1, the stands are coded Oaks, Conifers and Mixed conifer-oak. Which sites are mixed conifer oaks? or are these draw from a pooled dataset from all the sites grouped spatially?*

A: Sorry for this confusion, there are no mixed stands in the dataset. We were referring to the type of stands being compared in pairs to calculate the correlation coefficient between TRWi records (i.e., temporal coherence for site-pairs). The wording used in legend of Figure 1 (now Figure 2) has been modified to avoid such misunderstanding.

Q: *For a relatively simple analysis, the authors provide lots of references to appendices; four appendices, nine supplementary figures and three supplementary tables. This does not clarify the methods, rather it confuses the methods - it means that the reader needs to work very hard to work out what is relevant and what is not. It also hides fundamental details that should be placed front and center in the manuscript.*

A: We have simplified the information provided in Appendices. These have been reduced from four to one. The remaining Appendix 1 provides information on the

statistical approaches used to estimate synchrony values ($\hat{a}$) and correlations between TRWi and $\Delta^{13}C_i$ (r_Y) at the group level, which are not essential to follow the study but are probably relevant enough as to be included in the paper (and not just resort to published material on the topic). Also we have reduced the number of supplementary figures from nine to six. Fundamental details of the work are now included in the main text, particularly in the M&M section (i.e., relevant information of former Appendices 1 and 2).

Q: *To test these three hypotheses I suggest focusing the manuscript on the methods required and the analysis to support:*

1) a spatial analysis or map of synchrony in growth

2) a detailed examination of the relationship between D13C and TRWi in each taxa group

3) a spatial analysis or map of the strength/nature of the D13C:TRWi relationship

4) an analysis linking the frequency of warming induced drought stress and the D13C:TRWi relationship.

A: Thanks for the suggestion. We have included the following information in the manuscript:

- a map of synchrony in growth in Figure 1
- a map of the strength/nature of the $\Delta^{13}C$:TRW_i relationship in Figure 1 (insets)

The examination of the relationship between $\Delta^{13}C$ and TRW_i **at the taxa level** is not straightforward because many site chronologies of the same genus are distributed among different climate types and with site-pairs distances well over 1,000 km. This is especially evident for pine chronologies. However, in the case of oaks (eight site chronologies distributed among three climate types of central Europe) the joint analysis of the $\Delta^{13}C$ *vs*. TRW_i relationship has returned a value of +0.32 (±0.21), which follows the general pattern of positive relationships observed for all climate types except the Boreal one (Fig. 1). This information has been included in the text as to highlight the consistency of positive $\Delta^{13}C$ *vs*. TRW_i relations south of 60°N in Europe regardless of taxa (L. 401-403). Also, by excluding the site chronologies of the less represented genus at the group level from the calculations, the previously observed positive relations still hold true (albeit with higher SEs due to limited sample sizes):

1) Cold-continental (for *P. sylvestris*, excluding two *Q. robur* chronologies, *n*=3):
   r_Y = 0.20 (±0.18)
2) Temperate (for *Q. petraea*, excluding one *P. nigra* chronology, *n*=3):
   r_Y = 0.18 (±0.27)
3) Atlantic (for *Q. robur*, excluding one *P. sylvestris* chronology, *n*=3):
   r_Y = 0.35 (±0.25)
4) Mediterranean (for *Pinus* spp., excluding one *Cedrus atlantica* chronology, *n*=3):
   r_Y = 0.42 (±0.22)

Finally, we think that the analysis linking the frequency of warming induced drought stress and the $\Delta^{13}C$:TRW_i relationship is not obvious beyond the observation that

warming-induced drought stress increases over the 20th century in all climate types (perhaps with the exception of the Boreal climate). This can be seen in Fig. S6 (rise in temperature over time) and, also, in the analysis of trends in SPEI3 for June-August presented in Figure R3. Of course, we could perform a simple correlation analysis linking both variables, but this may not be concluding because of the spurious regression problem that arises when linking unrelated non-stationary variables. More refined statistical approaches, like a cointegration analysis (e.g. Shestakova et al. 2019), could be applied but we think this is beyond the scope of the study.

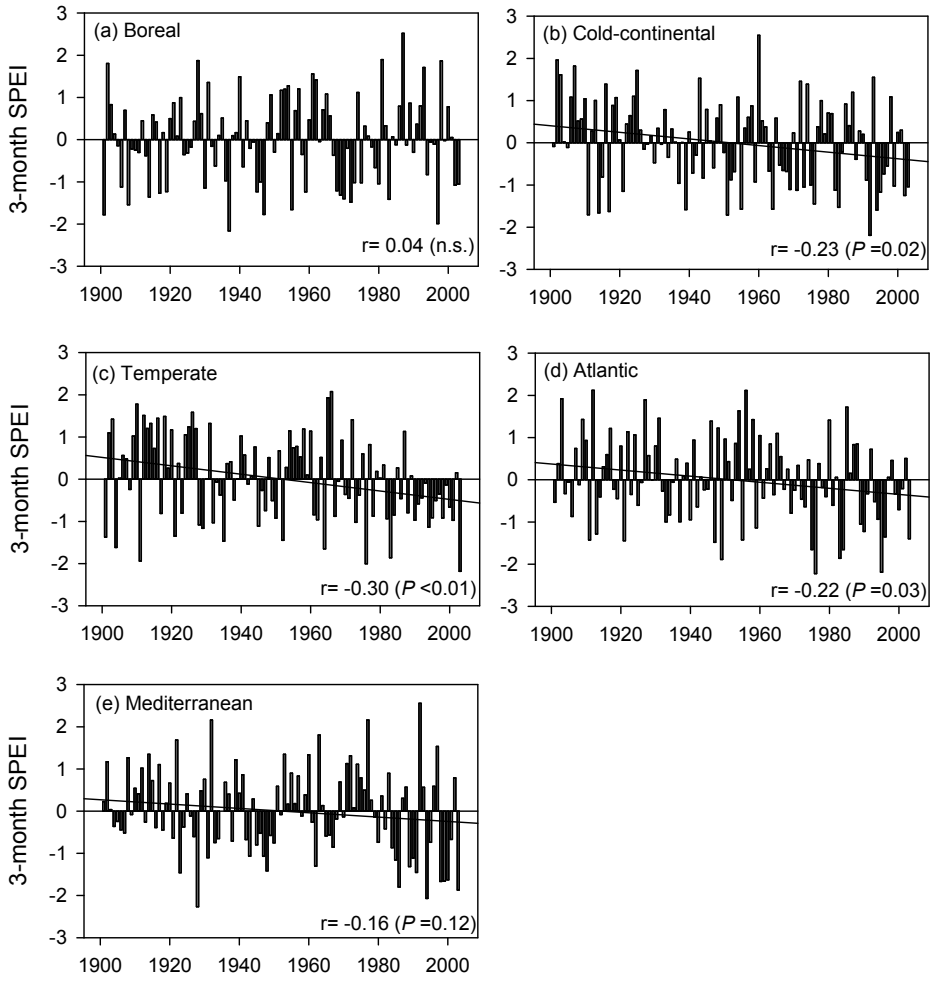

Figure R3. Trends in SPEI3 (June to August) for the different climate types examined in this study. Significant or marginally significant trends are represented by lines.

Specific comments:

Q: *20 sites or 20 chronologies? The abstract sounds like the authors have selected 20 old trees only.*

A: Each site represents one particular chronology made up of a number of trees (site mean = 46 trees; median = 28). To clarify this point, we make explicit mention to such 20 site chronologies in the Abstract.

Q: *Lines 136 – 144. The authors describe the calculation of BAI and then go on to talk about TRWi. Do the authors mean to define TRWi as BAI? If so the authors should state that clearly. If not TRWi should be clearly defined. I think that many in the tree ring community would assume that TRWi is a normalized index of tree ring width. The reader shouldn't have to to to the appendix for this important definition.*

A: We agree this is confusing. In this new version we have clearly separated the methodology used to obtain indexed records (TRW_i) from the approach used to calculate and interpret BAI trends (L. 195-203 for BAI). Indeed, these are two completely different ways to analyse radial growth records which we hope are perfectly clear now. The appendix referring to TRW_i calculations has been completely removed and the information incorporated into the main text following the suggestion of the reviewer.

Q: *Ring Width Increment may be a proxy for tree primary productivity, but it is not a direct one. Productivity is typically reported in gC per m2 which would not be a linear function of ring width (it would be cubic). In contrast d13C of wood is an integrated measure of canopy photosynthetic and fractionation processes - there are some caveats to correlating them. The authors have calculated BAI from the tree ring widths - I would expect a curvilinear relationship between BAI and d13C if stomatal control is being exerted on carbon gain. (BAI x height with tapor). Consider reviewing these concepts illustrated by Babst et al 2014, Dye et al 2016, Alexander et al 2017 and various other references.*

A: The reviewer is right in her/his expectation of BAI being non-linearly related to $\Delta^{13}C$. However, the variables that were examined and further (co)related to each other were not BAI and $\Delta^{13}C$. Instead, we used indexed tree-ring width (TRW_i) and indexed $\Delta^{13}C$ ($\Delta^{13}C_i$) values for this purpose. We apologise about this confusion, and we have tried to clarify this issue in this revised version (L. 287-289). Indexed records are calculated to provide new variables that are stationary (mean=1, constant variance). Therefore, the expectation of a curvilinear relationship no longer holds in this situation. The (linear) nature of the relationship between these two variables can be observed in Figure 1 (insets), which follows from a specific request of the reviewer asking for the strength / nature of the $\Delta^{13}C_i$:TRW_i relationship. The use of indexed ring-width records to understand $\Delta^{13}C$-based gas-exchange influences on radial growth through correlation analysis is reported in a number of articles focussing on the interpretation of the interannual relationship between radial growth and photosynthetic processes (Voelker et al. 2014; Del Castillo et al. 2015; Shestakova et al. 2017). In this way, it can be reasonably assumed that the relationships are free of age / size effects which are commonly associated to BAI trends.

Q: *Lines 153 – 157. The description of how classes were defined is a little ambiguous. I think I follow this but I suggest re-wording as much of the validity of the conclusions depend on these few lines of methods. Maybe describe how the groups were defined and then explain how pairwise tests were done?*

A: The statistical significance of pairwise correlations was assessed using the modified correlogram technique of Koenig & Knops (1998). To apply the statistical test, the distance classes must be defined beforehand. We chose a threshold of 500 km for the definition of consecutive distance classes as a compromise between number of classes and statistical power: the use of too many classes decreases the ability to detect significant pairwise correlations; conversely using too few classes decreases the chances to detect a significant distance class for spatially distant chronologies with a decent spatial resolution. The entire paragraph has been rewriting, and we hope the message has been improved (L. 239-250).

Q: *line 173 - suggest stating "consisted of 3-5 neighboring forest stands" rather than "a number"*

A: Done, thanks.

Q: *Line 187 - using a different co-variance model for each 'segment' requires explanation. Using 50 year increments to define the segments seems arbitrary. If something about these segments suggested that the relationship between TRWi and D13c should be different that would be preferable. Perhaps the authors have some reason for the selection of 50 year and the assumption that the relationship between D14C and TRWi should change? Did the authors move the 50 year window or was is defined as in line 221?*

A: The VCOV models used have been redefined for improving understanding of the different hypotheses being tested in each case (L. 270-278). Using different VCOV models for each segment allows detecting changes in data structure over time (L. 283-284), as it is in fact happening (Table S3). We chose a 50-year window to define the segments because it corresponds to about half of the study period (1901-2003). It is common practice to use moving windows of half the study period checking for stability in trait-trait or trait-climate relationships (e.g. Briffa and Jones, 1990; Carrer et al. 2010). Indeed, this is a good compromise between the length of the segment and the possibility to detect changes in the relationship over time. In any case, we tested an alternative segment of 30 years and the results are very much equivalent. The evolution of changes in â and r_Y was studied for successive 50-year segments lagged five years (Figs. 3 and 4). The statement in former L. 221 was inaccurate and has been dropped from the text.

Q: *Some of the observations in the paper could be influenced by species or genus specific stomatal behaviour (…).*

Oak species were characterized by anisohydric regulation of stomata

Pinus species exhibit isohydric behavior

A: The reviewer is right. However, a detailed analysis of the signal strength present in the isotopic data of the network reported no obvious species-specific differences (Treydte et al. 2007), with regional $\delta^{13}C$ and $\delta^{18}O$ chronologies sharing high common variance in year-to-year variations. Although the authors did not discuss the results in

terms of differential regulation of water loss between functional types, we presume that such consistency could arise from the focus put in the interpretation of high-frequency signals in the isotopic network, as also done in our study. Being such signals stationary, we speculate that the observed fluctuations share similar characteristics across taxa, regardless of their different original amplitude given by isohydric *vs*. anisohydric regulations. This reasoning has been included in L. 485-487.

Q: *Line 654 The tree-ring data used in this study are available upon request from the authors. I encourage the authors to contribute these data to some repository where they are discoverable and accessible. There are many dendrochronological data repositories available.*

A: Raw TRW records will be available at the International Tree Ring Database (ITRDB) provided the paper is published. $\delta^{13}C$ records are available as Supporting Information in Treydte et al. (2007), grl23621-sup-0003-fs02.eps file (freely accessible at https://agupubs.onlinelibrary.wiley.com/doi/full/10.1029/2007GL031106).

We have included this information in the Data Availability section of the manuscript.

References cited

Babst, F., Poulter, B., … & Frank, D. (2013). Site- and species-specific responses of forest growth to climate across the European continent. *Global Ecology and Biogeography*, **22**, 706–717.

Bréda, N., Cochard, H., Dreyer, E. & Granier, A. (1993). Field comparison of transpiration, stomatal conductance and vulnerability to cavitation of *Quercus petraea* and *Quercus robur* under water stress. *Annals of Forest Science*, **50**, 571–582.

Briffa, K., & Jones, P.D. (1990). Basic chronology statistics and assessment. In: Cook, E.R., and Kairiukstis, L.A., eds. Methods of dendrochronology: Applications in the environmental sciences. Dordrecht, The Netherlands: Kluwer Academic Publishers. 137−152.

Carrer, M., Nola, P., ... Urbinati, C. (2010). Contrasting tree-ring growth to climate responses of Abies alba toward the southern limit of its distribution area. *Oikos*, **119**, 1515–1525.

Carrer, M., Brunetti, M., Castagneri, D. (2016). The imprint of extreme climate events in century-long time series of wood anatomical traits in high-elevation conifers. *Frontiers in Plant Science*, **7,** 683.

Carrer. M., Castagneri, D., Prendin, A.L., Petit, G., von Arx, G. (2017). Retrospective analysis of wood anatomical traits reveals a recent extension in tree cambial activity in two high elevation conifers. *Frontiers in Plant Science*, **8,** 737.

del Castillo, J., Voltas, J., & Ferrio, J. P. (2015). Carbon isotope discrimination, radial growth, and NDVI share spatiotemporal responses to precipitation in Aleppo pine. *Trees*, **29**, 223–233.

Frank, D. C., Poulter, B., … Weigl, M. (2015). Water-use efficiency and transpiration across European forests during the Anthropocene. *Nature Climate Change*, **5**, 579–584.

Froux, F., Huc, R., Ducrey, M., Dreyer, E. (2002). Xylem hydraulic efficiency versus vulnerability in seedlings of four contrasting Mediterranean tree species (*Cedrus atlantica*, *Cupressus sempervirens*, *Pinus halepensis* and *Pinus nigra*). *Annals of Forest Science*, **59**, 409–418.

Girardin, M.P., Bouriaud, O., ... Bhatti, J. (2016). No growth stimulation of Canada's boreal forest under half-century of combined warming and CO_2 fertilization. *Proceedings of the National Academy of Sciences*, **113**, E8406–E8414.

Hargreaves, G. H., & Samani, Z. A. (1982). Estimating potential evapotranspiration. *Journal of the Irrigation and Drainage Division*, **108**, 225–230.

Hartl-Meier, C., Zang, C., Büntgen, U., Esper, J., Rothe, A., Göttlein, A., Dirnböck, T., & Treydte, K. (2015). Uniform climate sensitivity in tree-ring stable isotopes across species and sites in a mid-latitude temperate forest. *Tree Physiology*, **35**, 4–15.

Houslay, T.M., & Wilson, A.J. (2017) Avoiding the misuse of BLUP in behavioural ecology. *Behavioral Ecology*, **28**, 948–952.

Irvine, J., Perks, P., Magnani, F. & Grace, J. (1998) The response of *Pinus sylvestris* to drought: stomatal control of transpiration and hydraulic conductance. *Tree Physiology*, **18**, 393–402.

Koenig, W. D., & Knops, J. M. H. (1998). Testing for spatial autocorrelation in ecological studies. *Ecography*, **21**, 423–429.

Körner, C. (2015). Paradigm shift in plant growth control. *Current Opinion in Plant Biology, **25***, 107–114.

Ladjal, M., Deloche, N., Huc, R., & Ducrey, M. (2007) Effects of soil and air drought on growth, plant water status and leaf gas exchange in three Mediterranean cedar species: *Cedrus atlantica*, *C. brevifolia* and *C. libani*. *Trees*, **21**, 201–213.

Nabuurs, G. J., Lindner, M., Verkerk, P. J., Gunia, K., Deda, P., Michalak, R., & Grassi, G. (2013). First signs of carbon sink saturation in European forest biomass. *Nature Climate Change*, **3**, 792–796.

Pretzsch, H., Biber, P., Schütze, G., Uhl, E., & Rötzer, T. (2014) Forest stand growth dynamics in Central Europe have accelerated since 1870. *Nature Communications*, **5**, 4967.

Qiao, C-Y., Ran, J-H., Li, Y., & Wang, X-Q. (2007) Phylogeny and biogeography of *Cedrus* (Pinaceae) inferred from sequences of seven paternal chloroplast and maternal mitochondrial DNA regions. *Annals of Botany*, **100**, 573–580.

Saurer, M., Spahni, R., … Young, G. H. (2014). Spatial variability and temporal trends in water-use efficiency of European forest. *Global Change Biology*, **20**, 332–336.

Scheidegger, Y., Saurer, M., Bahn, M., & Siegwolf, R. (2000). Linking stable oxygen and carbon isotopes with stomatal conductance and photosynthetic capacity: a conceptual model. *Oecologia*, **125**, 350–357.

Shestakova, T.A., Gutiérrez, E., Kirdyanov, A.V., Camarero, J.J., Génova, M., Knorre, A.A., Linares, J.C., Resco de Dios, V., Sánchez-Salguero, R., Voltas, J., 2016. Forests synchronize their growth in contrasting Eurasian regions in response to climate warming. *Proceedings of the National Academy of Sciences*, **113**, 662–667.

Shestakova, T. A., Camarero, J. J., Ferrio, J. P., Knorre, A. A., Gutiérrez, E., & Voltas, J. (2017). Increasing drought effects on five European pines modulate Δ^{13}C-growth coupling along a Mediterranean altitudinal gradient. *Functional Ecology*, **31**, 1359–1370.

Shestakova, T. A., Gutiérrez, E., Valeriano, C., Lapshina, E., & Voltas, J. (2019). Recent loss of sensitivity to summer temperature constrains tree growth synchrony among boreal Eurasian forests. *Agricultural and Forest Meteorology*, **268**, 318–330.

Treydte, K., Frank, D. C., … Schleser, G. H. (2007). Signal strength and climate calibration of a European tree-ring isotope network. *Geophysical Research Letters*, **34**, L24302.

Voelker, S. L., Meinzer, F. C., Lachenbruch, B., Brooks, J. R., & Guyette, R. P. (2014). Drivers of radial growth and carbon isotope discrimination of bur oak (*Quercus macrocarpa* Michx.) across continental gradients in precipitation, vapour pressure deficit and irradiance. *Plant, Cell and Environment*, **37**, 766–779.